Review Article

Recent advances in zeolitic imidazolate frameworks as drug delivery systems for cancer therapy

Yuhan Wang [a,b], Yixin Tang [a], Lei Guo [a], Xi Yang [a], Shanli Wu [a,*], Ying Yue [b,*], Caina Xu [a,*]

[a] *Department of Biochemistry, College of Basic Medical Sciences, Jilin University, Changchun 130021, China*
[b] *Department of Gynecological Oncology, The First Hospital of Jilin University, Changchun 130021, China*

ARTICLE INFO

ABSTRACT

Biological nanotechnologies based on functional nanoplatforms have synergistically catalyzed the emergence of cancer therapies. As a subtype of metal-organic frameworks (MOFs), zeolitic imidazolate frameworks (ZIFs) have exploded in popularity in the field of biomaterials as excellent protective materials with the advantages of conformational flexibility, thermal and chemical stability, and functional controllability. With these superior properties, the applications of ZIF-based materials in combination with various therapies for cancer treatment have grown rapidly in recent years, showing remarkable achievements and great potential. This review elucidates the recent advancements in the use of ZIFs as drug delivery agents for cancer therapy. The structures, synthesis methods, properties, and various modifiers of ZIFs used in oncotherapy are presented. Recent advances in the application of ZIF-based nanoparticles as single or combination tumor treatments are reviewed. Furthermore, the future prospects, potential limitations, and challenges of the application of ZIF-based nanomaterials in cancer treatment are discussed. We except to fully explore the potential of ZIF-based materials to present a clear outline for their application as an effective cancer treatment to help them achieve early clinical application.

1. Introduction

Malignant tumors pose a major hazard to human health, causing millions of cancer deaths each year [1]. Traditional monotherapies such as surgery, chemotherapy, and radiotherapy have limited efficacy in treating malignant tumors and may cause severe side effects, including damage to healthy tissues, multidrug resistance (MDR), systemic toxicity, and complications [2]. The establishment and development of nanotechnology in conjunction with other treatments has provided new cancer therapy concepts. Emerging nanocarriers, such as liposomes [3], quantum

dots [4], inorganic mesoporous silica [5], metal-organic frameworks (MOFs) [6,7], and metal nanoparticles (NPs) [8], have been applied in preclinical or clinical studies of cancer therapy. These carriers improve the aqueous solubility, absorption, bioavailability, stability, and retention time of therapeutic agents *in vivo*. However, unmodified liposomes, quantum dots, inorganic mesoporous silica, and metal NPs do not exhibit stimuli-responsive release. In addition, to ensure the colloidal stability of inorganic NPs, an organic surface coating is generally required to avoid the adsorption of organic molecules on their surface [9].

MOFs with easily designed skeletons and adjustable pore sizes could be combined with liposomes, mesoporous silica, and metals via physical or chemical encapsulation to optimize nanomaterials by combining their advantages. Controllable nanocargos with high efficiency, low toxicity, and no or minimal side effects are being developed to treat malignancies. With the accomplishments of nanotechnology based on the enormous potential of nanocarriers in cell imaging and cancer treatment, nanocarriers, especially zeolitic imidazolate frameworks (ZIF)-based nanomaterials, will find more advantageous selection and amplification in the future.

As nanocarriers, MOFs are becoming increasingly prominent in industry and biomedicine due to their unique advantages, such as flexible synthesis, adjustable aperture, controllable dissociation, etc. [10]. MOFs are ordered porous coordination compounds consisting of metal ions or clusters interconnected with organic bridging ligands that are being developed to treat malignant tumors and have undergone remarkable development. ZIFs are a subgenus of MOFs and are composed of metal atoms and imidazolates. ZIFs exhibit extraordinary structures and high thermal and chemical stability [11,12]. Their tunable pore size makes molecular diffusion or mass transfer and the loading of large cargoes adjustable. Furthermore, macromolecular passive targeting and retention over prolonged periods are realized via enhanced permeability and retention effects [13]. Equipped with these attractive properties, ZIFs maintain the activities of biomolecules, reduce early leakage, and function with high agent loading and controllable drug release kinetics while avoiding immune clearance.

As one of the most representative types of ZIFs, ZIF-8 can degrade in a slightly acidic environment. The ZIF-67 core can offer more active reaction sites, and then the central Co^{2+}-catalyzed hydrogen peroxide (H_2O_2) decomposes to produce more O_2 and relieves tumor hypoxia [14]. Nanoscale ZIF-90, self-assembled via Zn^{2+} and imidazole-2-carboxaldehyde (2-ICA), is ATP-responsive and can be decomposed by an ATP-trigger, allowing it to target mitochondria [15]. With these properties, ZIFs have been considered for numerous applications, including catalysis [16,17], gas separation [18], sensing [19], and as biomaterial nanocarriers [20]. ZIFs have shown considerable potential in nanomedicine in recent years, especially in tumor nanomedicine treatment. Through rational design, ZIFs have been widely used to diagnose and treat malignant tumors in cell or animal models and have achieved remarkable results.
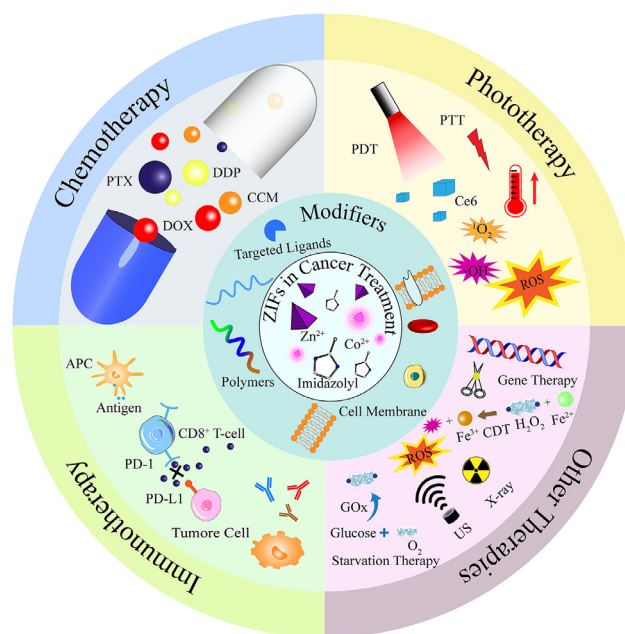

Fig. 1 – Schematic illustration of the use of ZIF-based nanomaterials in cancer treatment, including their synthesis, modification, and major tumor therapeutic applications.

With the rapid development of nanotechnology, especially the use of MOFs in tumor therapy, it is necessary to review and summarize their application in treating malignant tumors. The previous reviews mostly focused on a specific MOF or its application in a particular field, such as the biomedical use of MOF in DNA enzymes [21] or the use of ZIF in the treatment of breast cancer [22], or they classified and discussed different types of MOFs [23]. However, a comprehensive review of the use of ZIFs for antitumor therapy has not been performed over the past 2 years. This review highlighted the synthesis, properties, modification, and antitumor applications of ZIF-based nanocomposites in the antitumor field. The different stimulus responses and ionic and organic ligand properties of ZIF-based nanocomposites, including NPs (ZIF-7, ZIF-8, ZIF-67, ZIF-82 and ZIF-90 NPs), were systematically summarized. ZIFs can be modified by polymers, cell membranes, or targeted ligands. Herein, the current advancements in the use of different ZIFs in cancer therapy are outlined. As nanocarriers, ZIFs have been used mainly for chemotherapy, phototherapy, immunotherapy, chemodynamic therapy (CDT), starvation therapy, etc. (Fig. 1). First, a summary of ZIFs and their modifications in oncotherapy, including their structures, production techniques, and characteristics, is provided. Then, the potential of ZIF-based nanomaterials in cancer treatment, as well as any potential flaws or challenges, are recapped and discussed. Based on this review, it is expected that the potential of ZIF-based nanomaterials can be maximized, which paves the way for effective cancer treatment, the future development direction of ZIF-based nanomaterials can be determined, and safe and effective clinical applications can be realized as soon as possible.
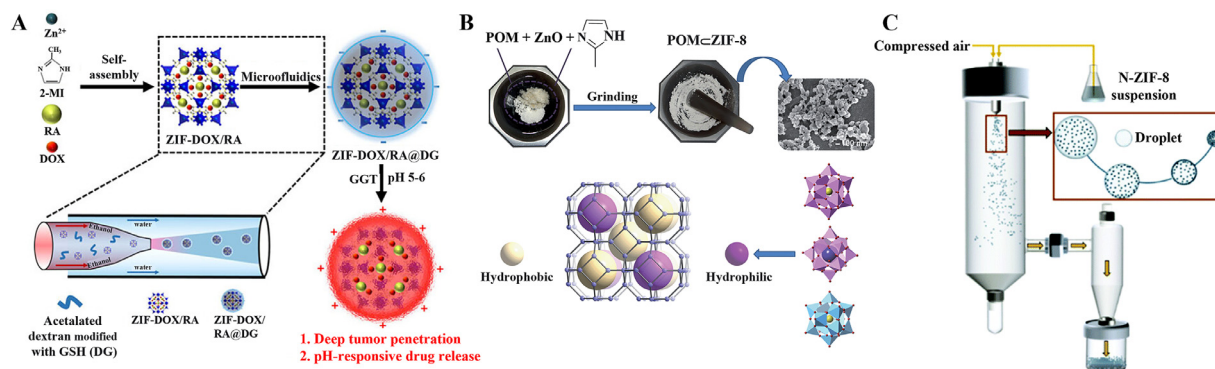
Fig. 2 – Schematic diagram of the preparation method for ZIFs. (A) Schematic of the microfluidic synthesis of ZIF-DOX/RA@DG. Reproduced from [25]. Copyright 2022 Wiley. (B) Schematic of the mechanochemical synthesis of POM⊂ZIF composites. Reproduced from [26]. Copyright 2014 Royal Society of Chemistry. (C) Schematic of the synthesis of HP-ZIF-8 via a spray drying system. Reproduced from [27]. Copyright 2022 Royal Society of Chemistry.

2. Synthesis, drug loading and properties of ZIFs

ZIFs are grown from $M(Im)_4$ tetrahedra (M: Zn^{2+} or Co^{2+}, Im: imidazolate) constructed by copolymerization between an imidazolate linker and cations [24], in which imidazolate bonds are connected by N atoms and provide tunable nanoscale ZIFs [11]. In this section, the synthesis methods of ZIFs and further comparisons of different encapsulation methods are presented. Furthermore, two main methods of cargo loading, the *in situ* encapsulation method and *ex situ* encapsulation, are discussed.

2.1. Synthesis and properties of ZIFs

Various strategies have been employed for constructing ZIF-based hybrids for cancer therapy, including solvothermal synthesis [28], the normal temperature stirring method [29], microfluidic synthesis [25,30], ultrasonic synthesis [31], mechanochemical synthesis [26], and spray drying [27]. Microfluidic synthesis, mechanochemical synthesis, and spray drying provide efficient and gentle preparation methods for ZIFs (Fig. 2). As drug carriers, synthetic conditions must be considered to avoid structural damage or degradation of molecules such as pharmaceuticals, enzymes, and nucleic acids. Integrated microfluidic synthesis precisely manipulates reactions on a micrometer scale and reduces the overall synthesis time [32]. Compared with solvothermal synthesis, mechanochemical synthesis improves the maximum uptake of some stable drugs by ZIFs [26]. Spray drying offers the apparent advantages of size control and high loading efficiency, but it also has the disadvantages of low thermal efficiency and a high initial installation cost [27]. Solvent-based static processes, especially ambient stirring techniques with green solvents, are increasingly popular in the cancer therapy field for ensuring human biosafety. The synthesis conditions of the ambient stirring method are simple and maneuverable with no requirement for additional instrumentation [33]. This method avoids the instability

or functional inactivation of the loaded drugs under high temperature, pH or light [34–36].

The morphology, pore size and particle size of ZIFs are affected by the synthesis conditions such as synthetic methods and properties [37]. Controllable ZIFs can be compounded by mixing metals, organic solvents, modulators, and templates [38]. The synthesis and characterization of nanoscale ZIFs were originally reported in 2009 [39]. ZIF-8 is one of the most representative ZIFs and comprises zinc nitrate (Zn) hexahydrate and 2-methylimidazolate (2-MIM). As reported, the formation of ZIF-8 includes four processes: nucleation, crystallization, growth, and stationary periods [40]. Organic ligands are less water soluble than ionic precursors, and hydrogen bonds between solveznts and precursors could interfere with nucleation [41]. ZIF-8 is synthesized by changing the ratios of ingredients, solvent types [such as methanol, deionized water, or N,N-dimethylformamide (DMF)], dosages, reaction times, surfactants, and temperatures [42]. When mixed in a methanol solution at room temperature, the molar ratio of 2-MIM to $Zn(NO_3)_2 \cdot 6H_2O$ affects the basic characteristics of ZIF-8, such as crystallinity, particle size, and porosity [43]. The average particle size of ZIF-8 decreased upon increasing the synthesis temperature [42] or 2-MIM/Zn molar ratio within a certain range [43]. Within certain bounds, increased pressure could increase the volume of ZIF-8 [44]. ZIF-8 is resistant to hydrolysis due to the hydrophobic apertures of ZIF-8, together with the strong bonding between the physical shielding of Zn^{2+} by four tetrahedrally coordinated 2-MIM linkers. The ZIF-8 framework is pH- and singlet oxygen ($^1O_2$)-responsive. Zn^{2+} and imidazolate ions could dissociate at an acidic pH [28,45], allowing the ZIF-8 framework to disintegrate and release cargos in an acidic environment while remaining stable under neutral or alkaline conditions, such as prolonged soaking in aqueous NaOH (8 M) at 100 °C [46].

The phototriggered $^1O_2$ could oxidize imidazole. This photosensitizer generates $^1O_2$ and subsequently converts imidazole to urea under light irradiation, leading to a dramatic increase in particle size and rapid cargo release [47]. ZIF-82 is composed of Zn^{2+}, 2-nitroimidazole (2-nIm), and 1H-

Table 1 – Summary of the synthesis of ZIF-based NPs for cancer therapy.

MOF type	Metal ions or clusters	Organic ligands	Solvent	Temperature	Stimulate	Refs.
ZIF-7	Zn^{2+}	Benzimidazole	DMF	Room temperature	pH	[53]
ZIF-8	Zn^{2+}	2-MIM	Methanol, ethyl alcohol, deionized water, DMF, or DEF	Room temperature or heat	pH, $^1O_2$, ultrasound sonication	[29,47,54,55]
ZIF-67	Co^{2+}	2-MIM	Methanol, deionized water, or DMF	Room temperature or 0 °C	pH	[14,29,56,57]
ZIF-82	Zn^{2+}	2-nIm, cnIm	DMF	Room temperature or heat	pH, hypoxia, UV, X-ray	[48–50]
ZIF-90	Zn^{2+}	2-ICA	DMF	Room temperature	pH, ATP	[15,58]

imidazole-4-carbonitrile (cnIm). The framework of ZIF-82 may cause nitro-nitrite isomerization under UV or X-ray irradiation [48,49]. The organic ligand of ZIF-82 acts as an electrophilic compound, endowing ZIF-82 with reduced glutathione (GSH) responsiveness under hypoxic conditions [50]. The framework of ZIF-90 can collapse in the presence of ATP, which indicates that the ZIF-90 carrier can target mitochondria [15].

The composition and properties of the ZIFs used for cancer treatment are summarized in Table 1. In addition, ZIF-9, ZIF-11, ZIF-68, ZIF-70, ZIF-78 and ZIF-79 have been investigated for their ability to load anticancer cargos [51,52].

2.2. Synthetic method for drug loading of ZIFs

In situ one-step encapsulation and ex situ two-step encapsulation methods are the two main methods for integrating cargos with ZIFs for further functionalizing ZIFs. The one-step method combines Zn^{2+} or Co^{2+}, imidazolate, and different cargos; cargos are added during the ZIF creation phase, and the ZIF structure forms around the entrapped molecule [29,45,59]. Cargos with unique functional groups (-COOH, -SO₃H, C=O, etc.) could interact and be satisfactorily encapsulated by ZIF-8. CCM@NZIF-8 (CCM: curcumin) was prepared using a straightforward and environmentally friendly one-step synthesis method, with an encapsulation effectiveness of up to 88.2 % [60]. Compared to in situ one-step encapsulation, cargos can also be brought into contact with previously created ZIF-8 via ex situ encapsulation. Compared with dissociated 5-fluorouracil (5-Fu), ZIF-8 loaded with 5-Fu by ex situ encapsulation showed favorable biocompatibility and prolonged blood circulation [61]. If the pore size of the ZIF is smaller than that of the guest molecule, then the loading molecule may remain on the surface of the ZIF through physical adsorption rather than entering the pores of the ZIF [58]. Therefore, based on the results above, in situ encapsulation, such as the encapsulation of caffeine [62], is more widely used because it is more common and convenient than ex situ encapsulation.

3. Modification of ZIF-derived nanocomposites

The therapeutic efficacy and cell fate of ZIF-based NPs are influenced by their physicochemical features (concentration, components, shape, charge, size, dispersity state, and solubility) [63,64]. Compared with polymeric or cell membranes, targeted and other modified ZIF-based materials, directly synthesized ZIF-based materials have poor dispersion, easy recognition and clearance by the immune system, and low accumulation in tumor areas [65,66]. Modifications to ZIF-based nanomaterials could improve their textural qualities and functional performance, improve cell internalization, minimize cytotoxicity, improve biocompatibility and stability, extend blood circulation time during in vivo transit, evade the immune system (avoid phagocytosis), and increase enrichment in the tumor region for enhanced therapeutic efficacy [67]. This section reviews the most commonly reported modifiers, including polymers, targeted agents, cell membranes and charge-reversal nanocarriers.

3.1. Modification of ZIFs by polymers

ZIFs modified with polymers exhibit remarkable properties, such as biocompatibility and minimal ZIF toxicity [68]. Poly(ethylene glycol) (PEG), polyvinyl pyrrolidone (PVP), polydopamine (PDA), polyethyleneimine (PEI), chitosan, and cell-penetrating peptide (CPP) are some of the polymer modification materials for ZIFs that are frequently utilized in oncotherapy.

PEGs are polymers with the ability to improve the biocompatibility of cargo, avoid aggregation, and prolong in vivo blood circulation time [69]. PEG prevents first-pass elimination of nanomaterials from the liver, spleen, reticuloendothelial system, and bone marrow and alters the surface charge of nanomaterials [70], but dense PEGylation might increase the hydrodynamic diameter and blood half-life, precluding the elimination of nanomaterials from the body [71]. ZIF-8 NPs modified by multiarm PEG with eight chemically reactive ends (8-arm-PEG) exhibited high colloidal dispersion and stability, and the particle size of the NPs could be adjusted by adjusting the temperature and the concentration of the 8-arm-PEG [65]. To improve the colloidal stability, control the release capacity of the NPs, and prevent them from aggregating, doxorubicin (DOX)@ZIF-8/PEG NPs were synthesized using monovalent amino PEG (PEG-NH₂) [72]. However, the PEG chain, end-group, and chemical nature of the PEG-acceptor core structure affect the immunogenicity of PEGylated drugs [73]. Anti-PEG antibodies may weaken these advantages or even result in more severe side effects by complement activation and cause faster

drug clearance (accelerated blood clearance phenomena) and hypersensitivity reactions, even leading to fatal anaphylaxis [73,74]. Therefore, screening patients for anti-PEG antibodies is necessary.

PVP is a nonionic, amphiphilic polymer that serves as both a surfactant and a capping agent. The weak coordination interactions between Zn^{2+} in ZIFs, the pyrrolidone rings (C=O) of PVP and the hydrophobic interactions between organic linkers in ZIFs and nonpolar PVP groups could increase the affinity for coordination-polymer spheres [75]. PVP stabilizes NPs in solvents during synthesis and controls pore penetration and the size and shape of certain NPs, whereas ZIF-82 NPs exhibit an inhomogeneous morphology without PVP [49]. PVP improved the stability of ZIF-67 in water for more than 1 week [56].

PDA is utilized to improve the biodegradability, biocompatibility, and biosafety of ZIFs [76]. PDA can be stimulated by near-infrared (NIR) light, which endows the nanomaterial with photothermal treatment properties. The photothermal conversion efficiency of PDA-PCM@ZIF-8/DOX was 30.61 % [76]. Curcumin-containing 2D nanosheets based on ZIF-8 with a PDA coating were designed to achieve precise and efficient tumor ablation [77].

In addition, other polymers, such as PEI, chitosan and CPPs, are also used to modify ZIFs. As a cationic capping agent, PEI endows nanomaterials with better loading and pH-responsive release capacity and stronger binding affinity to pDNA than nanomaterials without PEI [78]. Moreover, compared to those of pEGFP-C1@ZIF-8, the 25 kD structure of pEGFP-C1@ZIF-8-PEI enhanced cellular uptake due to better interactions with negatively charged cell membranes, which facilitated nanostructure binding and internalization, resulting in the expression of genes with high transfection efficacy [78]. Chitosan (N-acetyl-glucosamine-glucosamine copolymer) contains many amino and hydroxyl groups, is cationic, and can improve the pH sensitivity and biocompatibility of ZIF-based NPs [79,80]. CPPs can carry biologically active conjugates (cargos) into cells [81] and can be applied to ZIF-loaded nanomaterials via electrostatic forces and hydrogen bonds to improve tumor therapeutic effects [82]. ZIF-8 codelivered DOX and a CPP comprising histidine and arginine to aid endosome/lysosome escape, increased the cytotoxicity of the encapsulated drugs, and increased therapeutic delivery effectiveness [83].

3.2. Targeted modification carrier materials

To improve the tumor-targeting ability and utilization or uptake efficiency, targeted modification of ZIF-based NPs for tumor therapy is necessary. According to targeted sites, the targeted agents in this study, including tumor tissues, dendritic cells (DCs), tumor cell membranes, and tumor organelles, are summarized.

3.2.1. Targeting tumor tissues
RGD peptides can actively target tumor blood vessels by preferentially binding to the alpha(v)beta(3) ($\alpha_v\beta_3$) integrin, which is overexpressed during tumor neovascularization and is expressed at trace levels in normal cells [84]. Camptothecin (CPT)@ZIF-8 was modified with RGD (Arg-Gly-

Asp) by electrostatic interactions to form RGD@CPT@ZIF-8, which demonstrated superior targeting and enhanced cancer therapy performance [85]. RGD-modified drug delivery systems (DDSs), which consist of RGD, erythrocyte membrane, ZIF-8, and DOX, prolong blood circulation, enhance tumor-specific accumulation, and increase the tumor inhibition rate while minimizing adverse effects [86].

3.2.2. Targeting dendritic cells
The mannose receptor (cluster of differentiation number CD206) is a biomarker that is overexpressed by M2 macrophages, dendritic cells, and endothelial cells. Therefore, mannose could be exploited as a target carrier for nanodrug delivery for tumor treatment [87]. The (R837+1 MT)@ZIF-8-modified mannan achieved targeting of the surface of DCs [88]. Zhang et al. designed SC@ZIF@ADH, an acetaldehyde generator composed of ZIF-8, alcohol dehydrogenase (ADH), and *Saccharomyces cerevisiae* (SC) [89]. Mannose in the yeast cytoderm targeted tumor-associated macrophages and endowed the NPs with the function of targeted therapy.

3.2.3. Targeting tumor cell membranes
Tumor cell membranes contain various recognition sites. Ligand receptors such as hyaluronic acid (HA), folic acid, C-X-C chemokine receptor type 4 (CXCR4), and neuropeptide Y (NPY) can recognize and target functional proteins on the tumor cell membrane, improving the accumulation and cellular uptake of ZIF-based materials.

HA is a linear polyanionic natural polysaccharide. As a natural cellular receptor for HA, the differentiation 44 (CD44) cluster is a cell surface glycoprotein that is overexpressed on the membranes of various tumor cells [90]. HA can target CD44 in ovarian cancer, cervical cancer, colon adenocarcinoma, melanoma, and breast cancer [91–93]. The disaggregation of zinc cores (ZIF-8) achieved a dual gate-control system that realized both hyaluronidase (HAase) and pH responsiveness [94,95]. Wu et al. designed HZ@GD NPs containing a ZIF-8-loaded GLUT1 mRNA-cleaving DNAzyme (GD) tethered to HA to achieve systematic energy exhaustion by targeting melanoma cells via active CD44-targeting mechanisms [94]. Sun et al. developed an α-tocopherol succinate@ZIF-8 coating with HA. As an intelligent switch and tumor-targeted guide, the HA shell achieved tumor-specific accumulation and extended its blood circulation time [95].

Folate receptors (FRs) are transmembrane glycopolypeptides expressed on the cell surface with a high affinity for folic acid (FA). FR-α can target tumor cell membranes in malignancies, including ovarian and endometrial cancers [96]. Shi et al. designed FA-PEG/CQ@ZIF-8 NPs containing chloroquine diphosphate (CQ), an autophagy inhibitor, which showed more targeted features in HeLa cells than in HEK293 cells via the folic acid and folate receptors on HeLa cell membranes [70]. Qin et al. synthesized FZIF-8/DOX-PD-FA NPs composed of Gd-doped silicon NPs (Si-Gd NPs), chlorine e6 (Ce6), DOX, ZIF-8, poly(2-(diethylamino)ethyl methacrylate) polymers (HOOC-PDMAEMA-SH), and folic acid-PEG-maleimide (MaL-PEG-FA), which exhibited better cellular uptake by MCF-7 cancer cells than NPs without FA modification [97]. CXCR4 is a classical G protein-coupled receptor [98]. Cao et al. reported the tandem postsynthetic

modification of ZIF-7. The CXCR4 inhibitors benzimidazole-like inhibitor (Mavorixafor, AMD-070), 5-Fu and Mn^{2+} were loaded onto ZIF-7, and AMD targeted the CXCR4 receptor on the cell membrane and caused minor lung damage [53].

The NPY system is associated with malignancies such as neural crest-derived tumors, breast cancer, pancreatic cancer, and prostate cancer [99]. NPY analogs were used for peptide receptor targeting [100]. The G-protein coupled receptor Y1 receptor (Y1R) is overexpressed in triple-negative breast cancer (TNBC) tumors, suggesting that it could be used as a novel target in the treatment of TNBC [101]. The Y1R ligand [Asn^6, Pro^{34}]-NPY (AP) conjugated with nano ZIF-90 via facile postmodification improved the outcomes of TNBC treatment by targeting both breast cancer cells and mitochondria [58]. Jiang et al. developed manganese-ZIF-90 combined with the Y_1 receptor ligand [Asn^{28}, Pro^{30}, Trp^{32}]-NPY (25–36) (APT), which showed the ability to target the membrane and mitochondria of breast cancer cells, resulting in improved biocompatibility and MRI-guided tumor treatment efficacy [102].

3.2.4.   *Targeting tumor* cell nucleic acids and *organelles*

Nucleic acid aptamers are short oligonucleotides that can specifically bind to cognate disease biomarkers and be used to target ligands [103]. Sgc-8, a DNA aptamer, can target overexpressed human protein tyrosine kinase-7 in cancer cells, allowing receptor-dependent intracellular delivery [104]. The Sgc-8 aptamer-PDA-DOX/ZIF-8 improved the uptake efficiency of HeLa cells [105]. An aptamer (AS1411) combined with ZIF-8 and DOX targeted cancer cells, increased drug absorption, enhanced cancer therapy, and decreased side effects [106]. Balachandran et al. developed a versatile microfluidic approach to efficiently encapsulate ZIF-8 with different biomolecules, with aptamers (the DNA anti-CCL21 and A10 RNA aptamers, targeting lymph node and prostate cancer cells, respectively) modified on its surface, which showed greater accumulation in lymph nodes and tumor cells [32]. ZIF-90, which has a positive charge, can be decomposed by ATP and can actively target mitochondria in living cells via electrostatic interactions, which benefits drug delivery that worked on mitochondria [15,36]. ATP-responsive ZIF-90 carried cargos for tumor/mitochondria cascade targeting enriched atovaquone (AVO) in the mitochondria and inhibited tumor growth [107].

3.3.   *Cell membrane-camouflaged carrier materials*

Recently, emerging cell membrane biomimetic strategies have attracted much attention for facilitating the delivery of cargo by modifying nanomaterials, especially for cancer treatment [108]. Cell membrane biomimetic nanotechnology endows NPs with superior immune evasion, prolonged blood circulation, and targeting capacities to achieve bionic camouflage and drug delivery properties. The cell membranes designed to coat ZIFs are mainly derived from red blood cells (RBCs), cancer cells, and stem cells.

3.3.1.   *Erythrocyte membranes*

Membrane proteins such as CD47, decay-accelerating factor (CD55), CD59, membrane cofactor proteins, and complement receptor 1 allow RBCs to persist in human blood circulation for 120 days, preventing them from being eliminated by the immune system [109–111]. With biomimetic properties, the coated NPs imitate RBCs and interact effectively with the ambient environment, allowing them to accumulate in the tumor microenvironment (TME) via immune escape and achieve long-term blood circulation. Zhang et al. designed TGZ@eM NPs composed of ZIF-8, glucose oxidase (GOx), and the hypoxia-activated bioreductive prodrug 3-aminobenzotriazine-1,4-di-N-oxide tirapazamine (TPZ), which were cloaked with erythrocyte membranes to provide good biocompatibility in prolonged blood circulation [112]. Qiao and coworkers reported a biomimetic ZIF-based nanodrug (ZIF-8-DOX-LY-RM) consisting of a type 1 transforming growth factor β receptor (TGFBR1) inhibitor and DOX and coated it with an erythrocyte membrane, which possessed pH-responsive properties and exhibited prolonged blood circulation [113].

3.3.2.   *Cancer cell membranes*

Cancer cell membranes possess the characteristics of homotypic targeting and immune evasion. These membranes are coated on ZIF-based materials to achieve greater affinity for their donor cells and achieve precisely targeted tumor therapy [114]. Inspired by these advantages in cancer cells, Shao et al. designed AQ4N/GOx@ZIF-8@CM nanocomplexes, in which ZIF-8 was combined with hypoxia-activated bioreductive prodrugs [banoxantrone dihydrochloride (AQ4 N)], GOx and HepG2 membranes, whose uptake in HepG2 cells was greater than that in LO2 cells and RAW264.7 cells, and that preferentially accumulated in tumor areas, enabling targeted cancer starvation therapy and cascade-amplified chemotherapy [115]. Similarly, Zou et al. reported that ZIF-8@CAT@DOX biomimetic NPs composed of catalase (CAT), DOX and ZIF-8 coated with B16F10 cell membranes could accumulate in tumor tissues via homologous targeting, immune escape, and enhanced DOX accumulation on homologous tumor cells [116].

3.3.3.   *Other cell membranes*

The stem cell membrane exhibits tumor-targeting properties and decreased clearance of the cloaked nanocomposites by the immune system due to its low immunogenicity [117]. Liang et al. used stem cell membranes to wrap dexamethasone-loaded ZIF-8 [118], which exhibited excellent specific uptake of mesenchymal stem cells, high cytocompatibility, and enhanced osteogenesis. Nevertheless, monotypic cell membranes may not meet the omnifarious demands of cancer therapy. Hybrid membranes [119] may provide better efficacy and endow the ZIF-based nanomaterials with more properties in the future.

4.   ZIF-based NPs for cancer therapy

The design of ZIF-based cargos plays a role in consuming GSH [120] and lactate [121], producing reactive oxygen species (ROS) [122] in the TME, preventing premature release of cargos, etc. ZIF-NPs have strong bioadhesion and concentration- and time-dependent features [120,123].
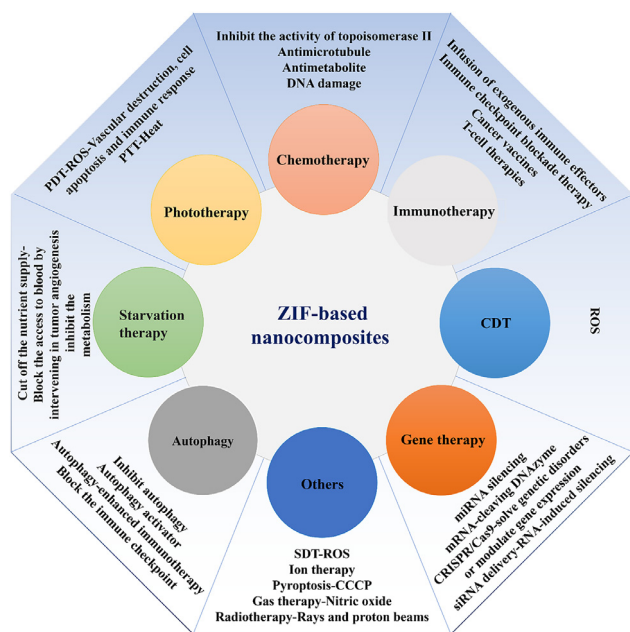
Fig. 3 – Schematic diagram of the classification and mechanism of ZIF-based NPs for cancer therapy.

Inspired by traditional healing methods, an increasing number of ZIF-based therapies, such as chemotherapy, phototherapy [including photothermal therapy (PTT) and photodynamic therapy (PDT)], immunotherapy, and CDT, are being used in tumor nanotherapy (Fig. 3). Based on the results presented to date, some representative ZIF-based tumor monotherapy and combined therapies in recent years are introduced and discussed below.

4.1.　Monotherapy

ZIFs exhibit attractive potential as frameworks for hybrid materials, and ZIF-based DDSs used in chemotherapy, phototherapy, immunotherapy, and other monotherapies for cancer treatment are described below (Table 2).

4.1.1.　Chemotherapy for cancer treatment
Chemotherapy is one of the most effective antitumor therapies and has various benefits, such as significantly slowed tumor growth and prolonged patient survival. At the same time, drawbacks such as allergic reactions, neurotoxicity, and bone marrow suppression cannot be ignored [134–136]. Chemotherapeutic agents such as DOX, 5-Fu, methotrexate (MTX), cisplatin (DDP), paclitaxel (PTX), gemcitabine, and CPT have been loaded in ZIFs [36,58,61,85,124,137], which are widely used in single-drug therapy or combination therapy. Through the encapsulation of ZIF, the toxicity of chemotherapeutic drugs to the blood system and normal cells is reduced.

DOX can inhibit the activity of topoisomerase II and damage DNA [138], and it has been widely loaded in ZIF-based NPs to treat cancer. Jiang et al. designed AP-ZIF-90@DOX, and the tumor inhibition rate of DOX loaded with ZIF-90 was significantly increased due to its dual responsiveness to high

ATP and low pH conditions and the targeted modification of AP [58]. With technology optimization, Yan and coworkers constructed hierarchically porous ZIF-8 via a spray drying-assisted process, and the drug loading efficiency and capacity of ZIF-8-loaded DOX reached 79 % and 79 %, respectively [27]. Chen et al. developed an intelligent hyaluronidase, pH, and glutathione multiple response nanogenerator, ZIF-8/DOX-HA@MIP, with a drug loading efficiency of over 88 %. This approach provided a simple and effective stimuli-responsive delivery system to enhance cancer therapeutic efficacy [139].

The antimetabolite drug 5-Fu inhibits thymidylate synthase and incorporates its metabolites into nucleic acids, exhibiting strong inhibitory effects on multiple cancer types [140]. Li et al. designed 5-Fu@ZIF-NPs, which entered cells partially via clathrin-mediated and macropinocytosis-mediated pathways, demonstrating the potential for delivery of 5-Fu via vehicles and bionano interactions, leading to pulmonary accumulation and improved therapeutic efficiency [123]. Jiang et al. developed pressure-induced amorphous ZIF-8 (aZIF-8) with high 5-Fu loading, demonstrating better tumor accumulation and therapeutic efficiency than ZIF-8/5-Fu, with a longer blood circulation time and slower drug release rate [61]. Foroushani et al. synthesized Mn_3O_4@PAA@ZIF-8/MTX NPs. MTX was immobilized onto the pH-sensitive system primarily through electrostatic interactions, which exhibited the ability of the T1 contrast agent to capture MCF-7 cells with high selectivity [124].

The chemotherapeutic agent platinum induces cell apoptosis via covalent binding to purine DNA bases; platinum-based cancer chemotherapy has been widely used for decades [141]. Nevertheless, the drug resistance and toxicity of platinum may affect its therapeutic efficacy. Xing et al. reported that ZIF-90@DDP NPs with dual pH and ATP responses targeting mitochondria showed greater cellular uptake and inhibition of nonresistant and DDP-resistant ovarian carcinoma cells than did free drugs [36]. Faraji Dizaji et al. used an electrospinning process to synthesize poly(lactic-co-glycolic acid) (PLGA)/chitosan/ZIF-8/PTX nanofibers, which achieved increased loading of PTX and sustained release. The nanofibers showed better performance in prostate cancer cell treatment by targeting and pH response [80]. Kamal et al. designed GEM⊂RGD@nZIF-8, which was more selective toward lung cancer cells because of the use of an autonomous homing peptide system, enhancing cellular uptake and increasing the number of apoptotic cells compared with that in normal cells [137]. Al-Jabbar and coworkers reported the use of BSA-Gem-Amy@ZIF-8/Dopa/GA, which encapsulated gemcitabine hydrochloride (Gem), amygdalin (Amy), PDA, and bovine serum albumin (BSA) into ZIF-8 chelated by Au^{3+} and conjugated via GA, which combined active and passive targeting and induced more MCF-7 cell apoptosis than gemcitabine alone [125]. After ZIF encapsulation, chemotherapy drugs have specific stimulatory responses on the TME, reduce toxicity to the blood system, and improve bioavailability through passive or active targeting.

4.1.2.　Phototherapy for cancer treatment
Inspired by the characteristics of the structure and controlled release of ZIFs in the acidic TME, the use of ZIF-loaded

Table 2 – Summary of ZIF-based nanocomposites applied in monotherapy cancer treatment.

MOF type	Loading materials	Nanocomplexes	Cells and animal models	Functionality	Refs.
ZIF-8	DOX	DOX@ZIF-8@AS1411	HeLa cells	Chemotherapy, targeting	[106]
	5-Fu	aZIF-8/5-Fu	ECA-109 cells, MCF-7 cells ECA-109 tumor-bearing mouse	Chemotherapy	[61]
	MTX, PAA	Mn_3O_4@PAA@ZIF-8/MTX	IMCF-7 cells	Chemotherapy, imaging	[124]
	PTX	PTX loaded-PLGA/chitosan/zeolite	LNCaP cells LNCaP tumor-bearing mice	Chemotherapy	[80]
	Gem, Amy	BSA-Gem-Amy@ZIF-8/Dopa/GA	MCF-7 cells	Chemotherapy	[125]
	$NaAsO_2$	AS@ZIF-8/PEG	HCC cells HCC-LM3 tumor-bearing nude mice	Chemotherapy	[126]
	CPT, RGD	CPT@ZIF-8@RGD	HeLa cells	Chemotherapy, targeting	[85]
	PA, TPP	UCNPs @ZIF+TPP+PA	4T1 cells Balb/c mice with 4T1 tumor xenografts	PDT	[127]
	Ce6	$^1O_2$-responsive (SR) micelles (mPEG-PAsp-IM-Zn^{2+}-Ce6)	4T1 cells 4T1 breast cancer model	PDT	[47]
	Cy5.5, ICG	Cy5.5&ICG@ZIF-8-Dex	A549 cells BALB/c mice bearing A549 tumors	PTT, imaging	[128]
	NV	NV-ZIF$_{MCF}$	Peripheral blood mononuclear cells isolated from patients with acute myeloid leukemia and chronic lymphoid leukemia 4T1 tumor-bearing mice	Immunotherapy, targeting	[129]
	KN046, 4-(trifluoromethyl)−1H-imidazole	KN046@^{19}F-ZIF-8	B16F10 cells the murine B16F10 melanoma BALB/c mice	Immunotherapy, ^{19}F MRI	[130]
	OVA, CpG, AlO(OH)	Aluminum adjuvant integrated CpG/ZANPs	EG7-OVA cells EG7-OVA cell tumor-bearing female C57BL/6 mice	Immunotherapy	[131]
	siRNA	siRNA-containing ZIF-8 (CAMEL-R)$_{HELA}$	HeLa cells HeLa cell tumor-bearing mice	Gene therapy, targeting	[114]
	CRISPR/Cas9	C^3-ZIF$_{MCF}$	MCF-7 cells MCF-7 tumor mouse models	Gene therapy, targeting	[132]
	ADH, SC	SC@ZIF@ADH	Murine colorectal cancer cells (CT26, ATCC CRL-2638) CT26 cell-bearing BALB/c mice	Acetaldehyde generator therapy, targeting	[89]
ZIF-67	PMS	PMS/ZIF-67	4T1 cells 4T1 breast cancer model	Immunogenicity	[133]
ZIF-90	DOX	AP-ZIF-90@DOX	TNBC cell line MDA-MB-231 with high overexpression of Y1R MDA-MB-231 tumor-bearing mouse	Chemotherapy, targeting	[58]
	DDP	ZIF-90@DDP	Human ovarian cancer cells A2780, DDP-resistant human ovarian cancer cells A2780/DDP	Chemotherapy, targeting	[36]
	AVO, hemin	iRGD/AVO−Hemin@ZIF-90	MDA-MB-436 cells MDA-MB-436 tumor-bearing nude mice	Mitochondrial metabolism, targeting	[107]

PAA, Polyacrylic acid; ICG, Indocyanine green; CpG, Cytosine-phosphate-guanine oligodeoxynucleotides; PMS, Peroxymonosulfate.

phototherapy agents promoted the development of combined cancer therapy strategies. Phototherapy is noninvasive and has fewer long-term side effects, and light irradiation, PDT and PTT can induce cell death by producing ROS or heating cells with phototherapy agents. ZIF-coated phototherapy agents can avoid nonspecific sensitization, direct exposure of phototherapy agents to the external environment such as the blood system, and light toxicity; reduce decomposition; and increase the stability of the photosensitizer before it reaches the tumor site [142]. NIR is widely used to diagnose and treat
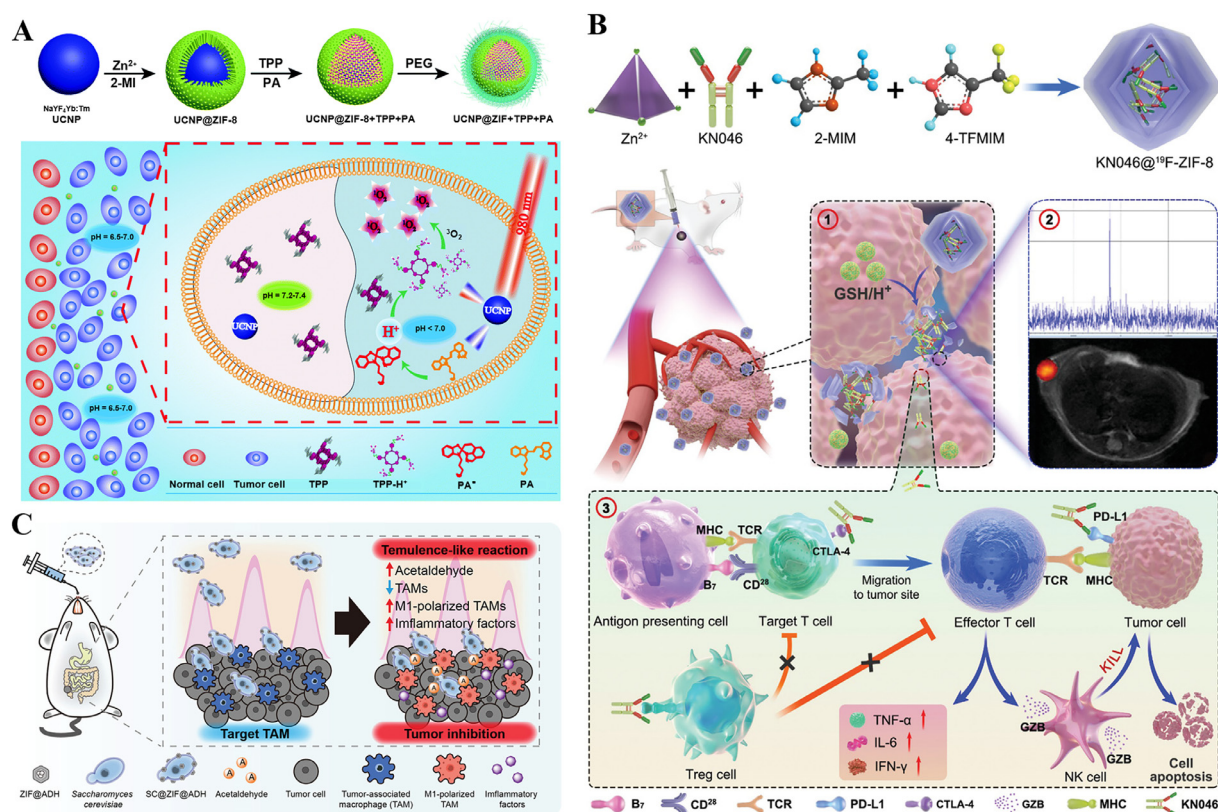
Fig. 4 – Schematic diagram of ZIF-based NPs for cancer monotherapy. (A) Schematic of the formation and anticancer mechanism of UCNP@ZIF+TPP+PA. Reproduced from [127]. Copyright 2020 Royal Society of Chemistry. (B) Schematic of the synthetic procedure and therapeutic mechanism of KN046@^{19}F-ZIF-8. Reproduced from [130]. Copyright 2021 Wiley. (C) Schematic illustration of SC@ZIF@ADH and the resulting temulencetemulence-like reaction to tumors. Reproduced from [89]. Copyright 2021 Wiley.

deep-seated tumors because light with longer wavelengths in the NIR region penetrates tumor tissues more deeply than normal tissues [143].

Photothermal transduction agents can convert light into heat energy, and then, the local overheating of the TME leads to the death of cancer cells. Wang et al. encapsulated ICG in ZIF-8. The PTT results indicated that ICG@ZIF-8 NPs detected tumors accurately and sensitively through fluorescence imaging and effectively induced local ablation under NIR [144].

Photosensitizers such as porphyrin can transform $^3O_2$ to $^1O_2$ and ROS in response to a particular light wavelength to kill cancer cells. Li et al. designed $^1O_2$-responsive (SR) micelles (mPEG-PAsp-IM-Zn^{2+}-Ce6). The $^1O_2$ generated under laser activation oxidizes imidazole to urea and causes micelle expansion, rapid Ce6 release, and cell apoptosis [47]. Wang et al. fabricated UCNP@ZIF+TPP+PA, composed of upconversion NPs (UCNPs), ZIF-8, a photoacid (PA) and an acid-responsive porphyrin (TPP), which was enhanced by coating the inner core of NaYF$_4$:Yb:Tm (UCNP) with ZIF-8 on the outside and loading both PA and TPP, restoring the intracellular pH microenvironment, destroying intracellular substances, and increasing $^1O_2$ production [127] (Fig. 4A). These hybrid nanocomposites provide promising ways to enhance cancer therapeutic efficacy.

4.1.3. Immunotherapy for cancer treatment

The use of immunotherapies, such as T-cell therapies, infusions of exogenous immune effectors, and cancer vaccines, is growing. ZIF-based nanomaterials can achieve target-controlled release through the EPR effect or active targeted modification and have shown attractive potential for combination with immunotherapy [129]. ZIF-based nanomaterials can simultaneously encapsulate antigens and adjuvants, synergistically amplifying the effect of immunotherapy [131].

Immune checkpoint blockade therapy (ICB) uses immune checkpoint inhibitors, such as cytotoxic T lymphocyte-associated antigen 4 (CTLA-4) and programmed death-1/programmed death ligand-1 (PD-1/PD-L1), to improve T-cell activity. Nivolumab (NV) is a monoclonal antibody checkpoint inhibitor. Alsaiari et al. designed an NV-ZIF coating with a cancer cell membrane, which showed greater efficacy than dissociative NVs, enabling tumor-specific targeted delivery and efficient activation of T cells in hematological malignancies [129]. Through rational design, ZIF combines immunization and imaging to achieve a theranostic nanoplatform. Song and his coworkers fabricated KN046@^{19}F-ZIF-8 (Fig. 4B), composed of KN046, a PD-L1/CTLA-4 antibody-Fc fusion protein, fluorine, and ZIF-8, which improved the immune response rate of antibody drugs in

melanoma immunotherapy, achieved CT/PET imaging and enhanced the efficiency of killing tumor cells [130].

Immunomodulatory factors, including the tumor-associated antigen ovalbumin (OVA), adjuvants (*e.g.*, CpG, AlO(OH), R837), and immunomodulators, can induce effective antitumor immune responses. Immunoadjuvants enhance the immune response by improving the recognition and delivery of tumor antigens via antigen-presenting cells. Zhong et al. developed a CpG/ZANP system that combined OVA, AlO(OH), and cytosine-phosphate-guanine (CpG, a Toll-like receptor 9 agonist) with ZIF-8 (hereafter ZANPs) and successfully induced strong humoral and cellular immune responses [131]. OVA loaded with ZIF decreased the cytotoxicity of OVA, and AlO(OH) increased the uptake of NPs by activating DCs. CpG was adsorbed onto the ZANP surface via electrostatic interactions to enhance cytotoxic T lymphocyte (CTL) responses. These hybrid ZIF-based nanocomposites provide a prospective way to develop versatile and efficient stimuli-responsive delivery systems for enhancing cancer therapeutic efficacy.

4.1.4. Other monotherapies for cancer treatment

In recent years, the application of ZIF-based nanomaterials to biological macromolecules, gene therapy, and mitochondrial metabolism has been increasing [21]. Based on the adapted biomimetic mineralization method, the encapsulation of single or multiple proteins in ZIF-8-based NPs enabled efficient protein codelivery and release and preserved the activity of the protein in living cells [145]. Proteins such as GOx encapsulated in ZIFs can achieve efficient cytotoxicity toward HepG2 cells by targeting the metabolism-redox circuit [146].

ZIF-8 markedly enhanced the efficacy of gene therapy [82]. Zhang created a biomimetic homotypic-targeting small interfering ribonucleic acid (siRNA)-containing ZIF-8 (abbreviated CAMEL-R)-coated HeLa cell membrane to achieve precise cancer therapy, extend circulation lifetime, promote efficient lysosomal escape of siRNAs, and induce effective tumor suppression [114].

As a genome-editing technology, clustered regularly interspaced short palindromic repeats (CRISPR)/associated protein 9 (CRISPR/Cas9) technology has been widely used to treat genetic disorders or modulate gene expression [147]. Nevertheless, its lack of targeting makes it less effective. Alyami and his coworkers modified CRISPR/Cas9 with homologous cell membranes and ZIF materials [132]. After bedecking, ZIF-8-loaded CRISPR/Cas9-covered MCF-7 cell membrane (C^3-ZIF$_{MCF}$)-transfected MCF-7 cells showed 3-fold repression of EGFP expression and 1-fold repression when transfected with C^3-ZIF$_{HELA}$. This novel strategy could open new avenues for drug delivery and treatment of heterogeneous tumors.

Through rational design, ZIFs can carry different drugs to achieve tumor metabolic reprogramming, reshape the tumor microenvironment, and achieve efficient treatment of tumors. Lu et al. reported iRGD/AVO–Hemin@ZIF-90 as a mitochondrial metabolism-targeted nanoplatform. Hemin can specifically degrade BACH1, a heme-dependent transcription factor, increasing the expression of the OXPHOS gene and changing mitochondrial metabolism, and AVO can inhibit the electron transport chain of OXPHOS. An ATP-responsive nanoplatform

with these two drugs was used to promote mitochondrial respiration in TNBC cells for tumor/mitochondria cascade targeting, resulting in reprogramming of the mitochondrial metabolism pathway in tumors [107].

In addition to intravenous injection, NPs can also be administered orally. Inspired by the method of percutaneous ethanol injection for tumor ablation, Zhang et al. designed the acetaldehyde generator SC@ZIF@ADH NPs [89] (Fig. 4C). ZIF-8-loaded ADH was attached to the surface of SC by electrostatic adsorption, and then the dissociated SC targeted M2 macrophages by mannose. The enrichment of ethanol produced by SC fermentation in hypoxic tumor areas was catalyzed to acetaldehyde by ADH. Acetaldehyde polarized M2 macrophages to M1 macrophages and induced tumor cell apoptosis and death.

In summary, ZIFs can be loaded with cargos of different solubilities, different photosensitivities, and different sizes, which endows these cargoes with antitumor effects via stimulation of release in response to specific triggers and additional functionalities, such as targeting or imaging, laying the foundation for the development of ZIF-based tumor nanotherapeutics.

4.2. Multiple combination therapies

Various ZIF-based monotherapies have been explored above. Chemotherapy treatments have a high cell-killing rate but can also harm normal cells or lead to MDR [148]. In addition, phototherapy may be restricted by insufficient penetration of deep tissue, TME hypoxia, phototoxicity, and photodecomposition under long-term light exposure [149]. Combined therapy could compensate for the limitations of single therapy and synergistically amplify the respective therapeutic effects, such as inhibiting the activity of P-glycoprotein [P-gp, a key protein encoded by MDR protein 1 (MDR1)] and heat shock protein 70 (HSP70), while overcoming the drug resistance of both chemotherapy and phototherapy [150]. The successful application of ZIF-based monotherapies has laid the foundation for multiple therapies based on ZIFs. Hence, we focused primarily on dual or multiple combination therapies (Table 3).

4.2.1. Chemotherapy-based combination therapy

In this section, synergistic chemotherapy-based combination therapies are discussed. Zhang et al. constructed DOX@ZIF-8/PVBP via an *in situ* synthetic strategy involving the use of a novel NIR-laser smart stimulus and enhanced its photothermal and chemotherapy properties to enhance its cancer therapeutic efficacy [173]. Whittaker et al. developed a switchable hydrophilicity fluoropolymer-MOF theranostic platform, ZIF-8-PFSAM-DOX, for cancer therapy [174]. This nanoplatform provides a prospective method to construct versatile and efficient stimuli-responsive delivery systems, laying the foundation for future clinical translation.

Hypoxia may reduce the cellular uptake of chemotherapy drugs and inhibit ROS production in tumor cells treated with chemotherapeutic drugs, reducing the efficiency of chemotherapy [176]. The problem of hypoxia in tumor tissue could be solved by the rational design of ZIF-based NPs. Chen et al. synthesized DOX-Pt-tipped Au@ZIF-8

Table 3 – Summary of ZIF-based nanocomposites applied in cancer treatment.

MOF type	Loading materials	Nanocomplexes	Cells and animal models	Functionality	Refs
ZIF-7	5-Fu, Mn^{2+}	AMD-ZIF-7(Mn)/5-Fu	K-150 cells K-150 cells BALB/c nude mice	Chemotherapy, MRI, targeting	[53]
ZIF-8	DOX	DOX-Pt-tipped Au@ZIF-8	4T1 cells 4T1 tumor-bearing mice	Chemotherapy, PDT, PTT	[151]
	DOX, ICG, bubble generator (NH_4HCO_3, ABC)	IDa-PRMSs@ZF	4T1 cells 4T1 tumor-bearing mice	Chemotherapy, PDT, PTT, targeting	[152]
	Rapamycin	Rapa@ZIF-8	Doxorubicin resistant MCF-7 cells (MCF-7/ADR cells) MCF-7/ADR-xenografted NOD/SCID mice	Chemotherapy, autophagy	[153]
	CCM	PDA-coated curcumin-involved 2D nanosheets (CMPD NSs)	HeLa, MCF-7 cells HeLa tumor-bearing mice	Chemo-photothermal-PAI	[77]
	Mitoxantrone (MIT), DNA demethylating agent hydralazine (HYD)	(M + H)@ZIF/HA NPs	4T1 cells 4T1 tumor model	Chemotherapy, apoptosis-pyroptosis-based immunotherapy	[154]
	Methylene blue (MB), CAT	PDA-MB-CAT-ZIF-8(PMCZ)	HeLa cells HeLa tumor-bearing mice	PTT, PDT	[155]
	CuS, aPD-1	CuS/Z@M$_{4T1}$	4T1 cells 4T1 tumor-bearing mice	PTT, immunotherapy, ion therapy, targeting	[156]
	Phycocyanin	MPEG$_{2000}$-ZIF/PC composites (PMs)	Patient-derived cancer cells (P^{3}DCC cells) bladder tumor tissue-derived PDX BALB/c nude mice mouse	PDT, alleviates intratumoral hypoxia	[157]
	PD-L1 siRNA, IR792, mesoporous carbon nanocomposite (MCN)	IR792-MCN@ZIF-8-PD-L1 siRNA(IM@ZP)	4T1 cells 4T1 tumor-bearing mice	PTT, gene therapy, immunotherapy	[158]
	Bromodomain-containing protein 4 (BRD4)-inhibitor (+)-JQ1 and iron-supplement ferric ammonium citrate -loaded gold nanorods (GNRs)	GNRs@JF/ZIF-8	4T1 cells 4T1 tumor-bearing mice	PTT, ferroptosis	[159]
	Ce6, DNAzyme	Ce6-DNAzyme@ZIF-8	MCF-7 cells MCF-7 tumor-bearing mice	PDT, gene silencing	[160]
	5-Aminolevulinic acid (ALA), DNAzyme	ALA&Dz@ZIF-PEG	MCF-7 cells MCF-7 tumor-bearing mice	PDT, immunotherapy, regulate metabolism, targeting	[161]
	GOx, chloroperoxidase (CPO)	GCZM	4T1 cells 4T1 tumor-bearing mice	Immunotherapy, starvation therapy, targeting	[162]
	g-C_3N_4-Au (CA)	CO$_2$-g-C_3N_4-Au@ZIF-8@F127 (CCAZF)	4T1 cells 4T1-bearing bilateral tumor model in BALB/c mice	Immunotherapy, gas therapy	[163]
	GOx, glucose transporter 1 (GLUT1) mRNA-cleaving DNAzyme	HZ@GD	B16F10 cells B16-F10 tumor-bearing C57BL/6 mice	Inhibit glycolysis, starvation therapy, ion therapy, targeting	[94]
	QCSG, HMME	QCSG/HA DA/ZDH(QH/ZDH)	H22 cells subcutaneous hepatic carcinoma (HCC) BALB/c mice	Sonodynamic therapy (SDT), hemostasis, targeting	[164]
	GSNO, Ce6	GSNO/Ce6@ZIF-8@Cytomembrane	4T1 cells 4T1 tumor-bearing mice	Gas-sonodynamic combined therapy, targeting	[165]

Table 3 (continued)

MOF type	Loading materials	Nanocomplexes	Cells and animal models	Functionality	Refs
ZIF-8, MIL-88B	DOX, MnOx	hM@ZMDF	MCF-7, HepG-2 cells	Chemotherapy, CDT, targeting	[166]
ZIF-8, ZIF-67	GOx, CuCo(O) nanozyme	CuCo(O)/GOx@PCNs	4T1 cells 4T1 tumor-bearing mice	PTT, immunotherapy, starvation therapy	[167]
ZIF-67	DOX, CuSe	ZIF-67@CuSe@PVP@DOX	4T1 cells 4T1 tumor-bearing mice	Chemotherapy, PTT	[56]
	DOX, CaO$_2$	CaO$_2$@DOX@ZIF-67	MCF-7 cells MCF-7 tumor-bearing mice	Chemotherapy /CDT	[57]
ZIF-82	–	ZIF-82-PVP	RM-1 cells RM-1 tumor-bearing mice	X-ray-induced nitrosative stress, autophagy	[49]
	Ferrous cysteine-phosphotungstate (FeCysPW), catalase DNAzyme (CAT Dz),	FeCysPW@ZIF-82@CAT Dz	HeLa cells HeLa tumor-bearing mice	CDT, redox dyshomeostasis strategy	[50]
	BER	UC-ZIF/BER	4T1 cells 4T1 tumor-bearing mice	Gas therapy, ion therapy	[48]
ZIF-90	DOX, DAPT	ZIF-90@DOX-HSA@DAPT-PEG-tLyP-1	HCCLM3 cells, CSCs enriched from HCCLM3 cells HCCLM3 xenograft model	Chemotherapy, deep tumor-penetrating	[168]
	5-Fu	APT-Mn-ZIF-90/5-Fu	MCF-7 cells MCF-7 tumor-bearing mice	Chemotherapy, MRI, targeting	[102]
	Gem, IR780, Pt	Pt@ZIF-90@Gem@IR780 nanoplatforms (denoted as PZGI NPs)	BxPC-3 cells BxPC-3 tumor-bearing mice	Chemotherapy, SDT, targeting	[169]
	MB, *Shewanella oneidensis* MR-1	PTB@ZIF-90/MB	CT26 cells CT26 tumor-bearing mice	PTT, PDT	[170]
	Ce6, CaO$_2$, Fe	CaO$_2$@ZIF-Fe/Ce6@PEG	4T1 cells 4T1 tumor-bearing mice	PDT, CDT	[171]
	RNase A-NBC, CRISPR/Cas9	ZIF-90/RNase A-NBC	HeLa cells	Protein therapy, gene therapy	[172]

[151]. Pt-tipped Au NR heterostructures with catalase-like activity improved the O$_2$ level in the TME and showed outstanding photothermal/photodynamic properties via efficient plasmon-induced electron-hole separation under 1064 nm laser irradiation. The nanosystem achieved synergistic chemo-phototherapy with bimodal imaging, and the treatment outcomes were mutually reinforced. Through the rational design of ZIF-based hybrid structures, hypoxia in the TME can be alleviated by combination therapy, which synergistically enhances the effect of chemotherapy. Zou et al. reported a ZIF-8@CAT@DOX(ZCD)-coated homologous membrane (abbreviated as mZCD) nanosystem in which O$_2$ was supplied by CAT to ameliorate the anoxic TME and downregulate the expression of hypoxia-inducible factor 1α. mZCD combined with αPD-1 inhibited PD-1/PD-L1 and recruited more infiltrating CD8+ T cells and antigen-presenting cells to induce a stronger immune response, which further improved the effectiveness of the synergetic chemotherapy and immunotherapy [116]. The TGFBR1 inhibitor LY364947 (LY) can reduce the expression of collagen I to regulate the tumor extracellular matrix. Qiao et al. constructed the biomimetic nanocomplex ZIF-8-DOX-LY-RM for increased cellular uptake, collagen depletion, enhanced

penetration, and increased O$_2$ supply to alleviate hypoxia, which subsequently relieved chemoresistance (Fig. 5A) [113].

In addition to providing O$_2$ to ameliorate hypoxia in the TME, researchers have used hypoxia to activate nanoagents. Fang et al. developed ZnS@ZIF-8/ICG/TPZ (ZSZIT) for H$_2$S-sensitized cascade PDT/chemotherapy. The released ICG triggered ROS under NIR irradiation and consumed O$_2$; H$_2$S produced by ZnS cores suppressed CAT expression and promoted hypoxia in the TME. Then, the hypoxia-activated bioreductive prodrug TPZ exerted cytotoxic effects in tumor areas with minimal damage to normal cells [177]. ZIF-8-based GOx combined with hypoxia-activated bioreductive prodrugs, such as TPZ [112] and banoxantrone dihydrochloride (AQ4 N) [115], exacerbated the hypoxia of the TME and subsequently cascaded the amplification of hypoxia-induced chemotherapeutic toxicity, significantly inhibiting tumor growth.

The combination of ZIF-mediated regulation of the tumor cell oxidation balance, drug penetration, autophagy, and/or tumor angiogenesis with chemotherapy has also shown potential for the treatment of a wide range of tumors. DOX is the most commonly used chemotherapeutic drug encapsulated within ZIFs, which not only exploits its
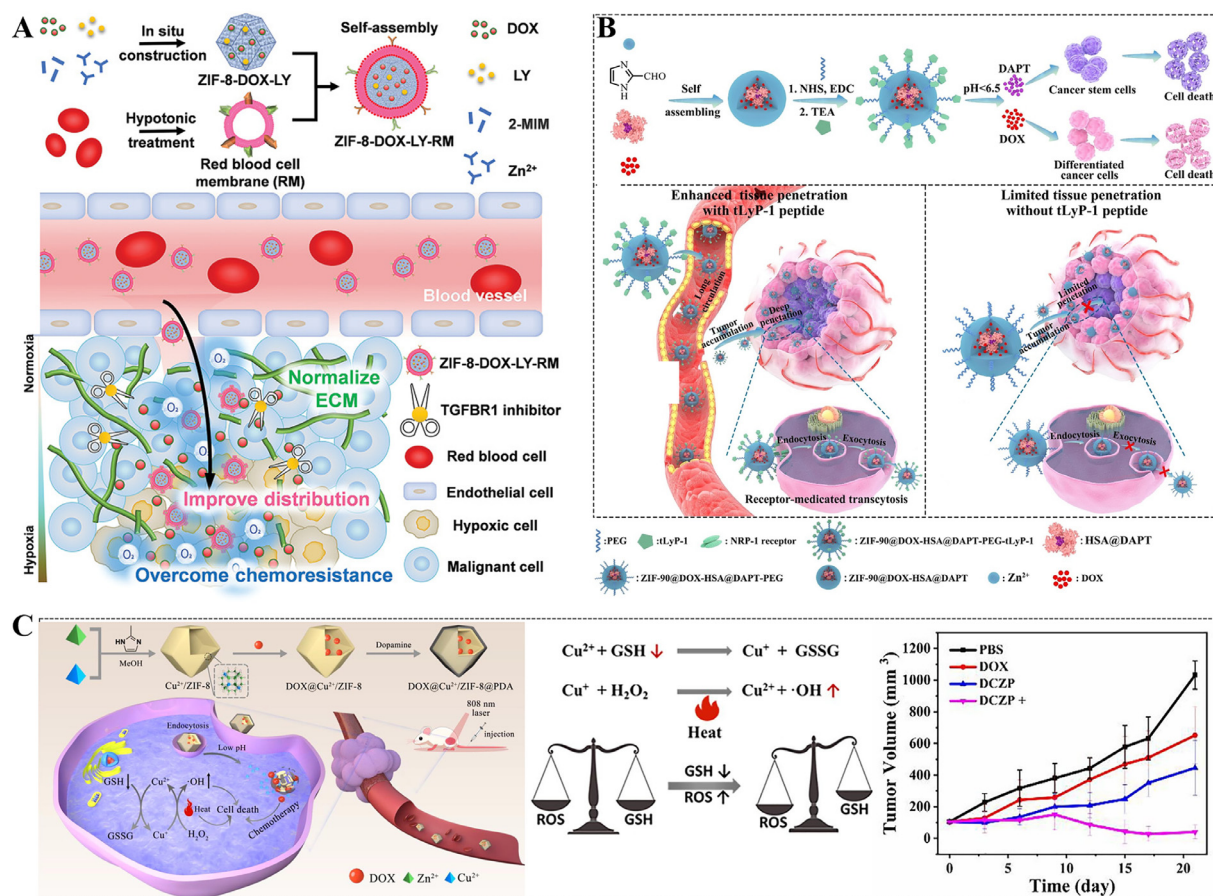
Fig. 5 – Schematic diagram of ZIF-based NPs for chemotherapy-based combination therapy. (A) Schematic diagram of the synthesis of ZIF-8-DOX-LY-RM NPs and the enhanced delivery and therapeutic efficacy of ZIF-8-DOX-LY-RM NPs. Reproduced from [113]. Copyright 2022, Wiley. (B) Schematic of the preparation process and curative mechanism of the ZIF-90@DOX-HSA@DAPT-PEG-tLyP-1 nanosystem. Reproduced from [168]. Copyright 2021 Elsevier. (C) Illustration of the preparation procedure, mechanism of DCZP, and tumor growth curves of mice subjected to different treatments. Reproduced from [175]. Copyright 2022 Elsevier.

inherent fluorescence and DNA damage properties but also allows for combination therapy. Chen et al. found that NPs composed of ZIF-90-loaded DOX, tumor-penetrating peptide (tLyP-1), and N-[N-(3,5-difluorophenacetyl)−1-alanyl]-S-phenyl glycine t–butyl ester (DAPT) achieved deep tumor penetration and long blood circulation times, and eradicated both differentiated cancer cells and cancer stem cells (CSCs) [168] (Fig. 5B). Wang et al. constructed a ZIF-based nanocomposite (DOX@Cu^{2+}/ZIF-8@PDA, DCZP) to achieve a combination of a Cu$^+$-catalyzed Fenton-like reaction, GSH depletion, chemotherapy, and PTT [175] (Fig. 5C). This method offers a new way to construct versatile and efficient stimuli-responsive delivery systems for chemotherapeutic agents to enhance cancer therapeutic efficacy. Xu and coworkers reported that rapamycin-encapsulated ZIF-8 (Rapa@ZIF-8) and DOX showed remarkable therapeutic efficacy by interfering with the mTOR pathway and autophagy for adjunct chemotherapy [153]. Tan et al. designed a multifunctional injectable ZIF-based nanohybrid, Dox/Cel/MOFs@Gel, in which Dox and celecoxib (Cel)

were coloaded into ZIF-8 integrated with thermosensitive hydrogels, achieving efficient synergistic oral cancer therapy by dual drug release, inducing cell apoptosis and inhibiting angiogenesis [178].

Drug resistance is a major challenge in achieving effective chemotherapy [179]. The ATP-binding cassette (ABC) transporters P-gp and ABCG2 can act as transmembrane drug efflux pumps to reduce the accumulation of intracellular drugs, which leads to acquired chemotherapeutic resistance [180]. Hence, to some extent, inhibiting the function of P-gp could reverse MDR. Liu et al. established MPDA@ZIF-8/DOX+GOx, in which the mesoporous PDA (MPDA) core was loaded with DOX while the ZIF-8 shell was coated with GOx. The nanosystem achieved effective codelivery and sequential release of GOx and DOX, consumed glucose for ATP deprivation, suppressed ATP-dependent drug efflux, and increased the accumulation of DOX in tumors, which significantly improved its anticancer effects [181].

The development and integration of emerging technologies offer new prospects for tumor treatment.
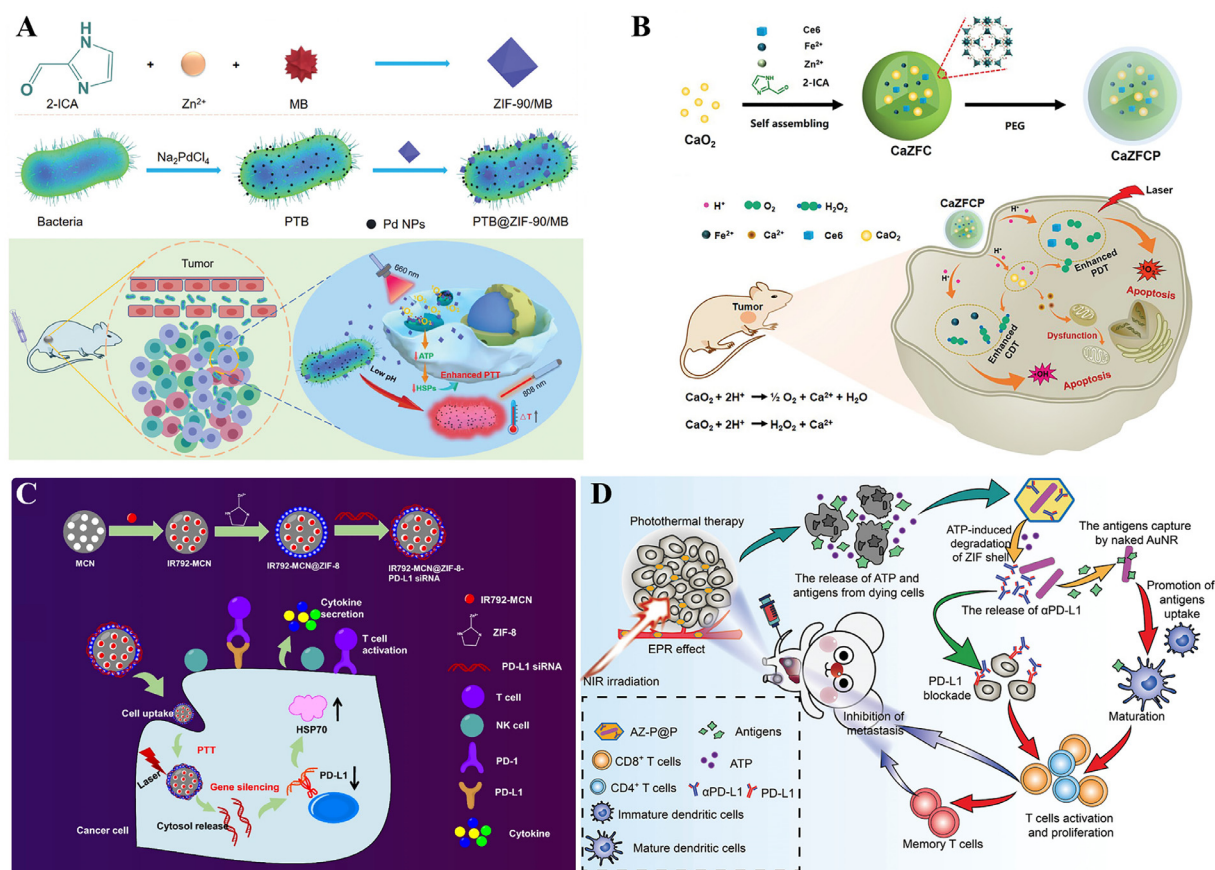
Fig. 6 – Schematic diagram of ZIF-based NPs for phototherapy-based combination therapy. (A) Schematic of the formation of ZIF-90/MB, the synthetic procedure of PTB and PTB@ZIF-90/MB, and the mechanism of PTB@ZIF-90/MB in cancer therapy. Reproduced from [170]. Copyright 2020 Wiley. (B) The synthesis and mechanism of CaZFCP for enhanced CDT/PDT. Reproduced from [171]. Copyright 2021 Wiley. (C) The synthesis and mechanism of IM@ZP. Reproduced from [158]. Copyright 2022 BMC Part of Springer Nature. (D) Schematic illustration of the improvement of tumor immunotherapy by AZ-P@P. ATP and TDPAs are released after PTT. An αPD-L1 antibody blocks the interaction between PD-L1 on tumor cells and PD-1 on T cells, inhibiting tumor metastasis. Reproduced from [184]. Copyright 2020 Wiley.

Wang et al. devised a combination of 3D printing and ZIF materials for the treatment of osteosarcoma. ZIF-8 was applied to encapsulate DOX and IDO inhibitors, which were then integrated into 3D-printed titanium scaffolds. The resulting Ti-ZIF-8@DOX-IDO (TZDI) exhibited specific microwave thermal performance under microwave irradiation and enhancement of its chemotherapeutic and immunotherapeutic activity for eradicating orthotopic osteosarcoma [182]. Overall, these hybrid nanocomposites provide simple yet powerful methods to improve stability and biosecurity, prevent unwanted clearance, and reduce the side effects of chemotherapeutic agents.

4.2.2. Phototherapy-based combination therapy

Combining photosensitizers and photothermal agents, the synergetic therapy of ZIF-based composites with PDT and PTT showed dual functions and enhanced therapeutic effects. Occasionally, it was challenging to have the same maximum absorption wavelengths of PTT and PDT agents in the NIR region, with insufficient penetration through tissues by NIR radiation, which may result in therapeutic failure [143]. Chen et al. fabricated PTB@ZIF-90/MB NPs [170] (Fig. 6A). The ability of the living photothermal bacterium *S. oneidensis* MR-1 to biomineralize palladium NPs on its surface hybridized with ZIF-90/MB to release MB into the mitochondria, disrupting mitochondrial redox hemostasis by producing $^1O_2$ under combined 660 nm light and an 808 nm laser, inhibiting ATP production and downregulating HSP expression significantly improved the treatment efficiency of targeting and heat tolerance in PTT. Phototherapy, in combination with other therapies, can help compensate for this shortfall. Feng's group used ZIF-8 to encapsulate PDA, CAT, and the photosensitizer MB to construct a tumor acidic pH-triggered nanoplatform. CAT-mediated self-sufficient O_2 generation could ameliorate hypoxia in the TME, resulting in synergistic O_2-enhanced PDT-PTT, which showed excellent therapeutic efficacy [155].

Hypoxia and inhomogeneous heat dispersion, among other factors, may reduce the effectiveness of individual phototherapy [142]. Shen et al. designed CaO$_2$@ZIF-Fe/Ce6@PEG (CaZFCP) to enhance the efficacy of PDT/CDT by providing H_2O_2 and O_2 produced by CaO$_2$ and then delivering more hydroxyl radicals ($\cdot$OH) and $^1O_2$. In addition,

Ca^{2+} overload amplified intracellular oxidative stress and caused mitochondrial dysfunction, which further improved the efficacy of combined CDT/PDT [171] (Fig. 6B). Wang et al. designed a nanozyme composed of double-layered ZIF-8@ZIF-67, porous carbon, CuCo(O), and GOx through pyrolysis, calcination, mixing, and stirring as an oxygen supply, glucose consumption, and PTT nanoplatform with 40.04 % photothermal conversion efficiency. CuCO(O) produced O_2 and promoted GOx to enhance starvation therapy. This system could not only ablate primary tumors via PTT and starvation therapy but also induce a systemic immune response to kill distal tumors via synergistic therapy [167]. The authors also constructed a Fe_3O_4@ZIF-8/GOx@MnO_2 multilayer core-shell nanostructure. MnO_2 catalyzed inner H_2O_2 to produce O_2 to provide reaction raw materials for GOx. The generated H_2O_2 and gluconic acid produced by GOx enhanced the Fenton reaction efficiency of Fe^{2+}. Moreover, PTT promoted the oxidase activities of MnO_2 and GOx and the catalase-like properties of Fe^{2+}. The hybrid nanozyme facilitated M2-type macrophages to transform into the M1-type, realizing a combination of PTT, immunotherapy, CDT, and starvation therapy [183].

In addition to supplying O_2 to the tumor site to alleviate intratumoral hypoxia, reducing intratumor oxygen consumption via the mitochondrial complex I inhibitor papaverine provided another way to enhance the effectiveness of phototherapy. Chen et al. encapsulated phycocyanin (PC), a water-soluble, surface charge negative photosensitizer agent, into ZIF-8 to form $MPEG_{2000}$-ZIF/PC composites (PMs), which inhibited mitochondrial respiration via the use of papaverine to augment the efficacy of PDT [157].

The combination of phototherapy and immunotherapy through ZIFs also provided new ideas for tumor treatment. 1-Methyl-D-tryptophan (1MT), an immunoregulatory enzyme (indoleamine 2,3-dioxygenase) inhibitor, can increase the ratio of effector T cells to regulatory T cells, preventing immune evasion. Zhang et al. designed dual tailor-made ZIF NPs in which ZIF-8-encapsulated indocyanine green (IR820) (HA/IR820@ZIF-8) acted as a PTT targeting agent and ZIF-8 encapsulated 1 MT, the adjuvant imiquimod R837, and mannan (MAN) (MAN/(R837+1 MT)@ZIF-8) acted as a targeting agent to target the surface of DCs. Synchronous intravenous injection of HA/IR820@ZIF-8 and MAN/(R837+1 MT)@ZIF-8, tumor autoantigens generated after PTT combined with immune adjuvants, promoted systemic antitumor immunity, specifically inducing immunogenic cell death (ICD), which could amplify the synergistic therapeutic effect of immune response activation and immune escape by actively targeting tumors and DCs [88]. Wang and his group synthesized IR792-MCN@ZIF-8-PD-L1 siRNA (IM@ZP) NPs via *in situ* synthesis and physical adsorption [158]. With NIR laser irradiation, the photothermal molecules mesoporous carbon nanocomposite (MCN) and IR792 enhanced the photothermal conversion ability and decreased cell viability. The released siRNA downregulated the expression of PD-L1. IM@ZP upregulated HSP70 expression, induced DC maturation and cytokine secretion, effectively killed 4T1 tumor cells, inhibited lung metastasis, and amplified the effect of photothermal immunotherapy via PD-L1 gene silencing (Fig. 6C). Cheng et al.

constructed AZ-P@P by integrating gold nanorods (AuNRs) as cores and the outermost ZIF-8 shell carrying αPD-L1. After PTT, the AuNRs captured the tumor-derived protein antigens (TDPAs) released by the dead cells, facilitated the uptake of TDPAs by DCs, and promoted the intratumoral infiltration of CTLs. The released αPD-L1 promoted the activation and proliferation of T cells. AZ-P@P achieved highly effective antitumor immunotherapy after local PTT via NIR irradiation destroyed primary tumors and suppressed metastatic tumors [184] (Fig. 6D). The metabolic regulator lonidamine (Lon) can block the hexokinase signaling pathway, reduce lactate secretion, and disrupt metabolic homeostasis. By coencapsulating Ce6 and the metabolic regulator Lon with ZIF-8 and modifying the homotypic 4T1 tumor cell membrane, biomimetic multifunctional NPs were designed to regulate tumor metabolic abnormalities and enhance PDT-mediated immunotherapy to synergistically enhance tumor ablation. CM-ZIF8@Ce6/Lon can consume lactate, relieve hypoxia, and reverse immunosuppression in the TME [185].

Overall, PPT or PDT based on ZIF nanomaterials can trigger ICD and achieve mutually reinforced cancer treatment when combined with immunotherapy. Wang et al. designed a TME-activated biomimetic fluorescence imaging and photothermal imaging nanoplatform, Z-M-LA@CM, with the property of an "off-on" fluorescence response toward GSH, enabling multimodal imaging, self-enhanced PTT/CDT synergistic therapy, and immune effects [186].

4.2.3. Immunotherapy-based combination therapy

Traditional immunotherapy has several disadvantages, such as off-target toxicity, a low immune response, and poor tumor infiltration [187]. Zhang et al. designed artificial "super neutrophils," composed of GOx, chloroperoxidase (CPO), and neutrophil membrane (NM)-modified ZIF-8, which achieved inflammation targeting and hypochlorous acid (HClO) generation via enzymatic cascades, to eradicate tumors [162] (Fig. 7A). Artificial "super neutrophils" generated seven times more reactive HClO than did natural neutrophils. Cai et al. first encapsulated Cu_{2-x}Se and a ferroptosis agonist (erastin) into nanoZIF-8 and then coated the ZIF-8 shell with PEG and FA to obtain Cu_{2-x}Se/ZIF-8@Era-PEG-FA. These multifunctional polymer-ZIF hybrids provided improved biocompatibility and controllable release, enabling ferroptosis activation and immunotherapy to enhance cancer therapeutic efficacy [188]. The self-supplying nanoreactors offered a novel strategic synergy of multifunctionalities.

The combination of ICD, ICB, and other effective tumor therapies has shown promise in nanomedicine-based tumor therapy. Excessive ROS can cause intense oxidative stress and induce ICD in tumor cells. Xiao and his coworkers designed a multifunctional carbon monoxide nanogenerator. CO_2-g-C_3N_4-Au@ZIF-8@F127 (CCAZF) exhibited simultaneous photocatalytic gas therapy under the stimulation of pH, NIR and anti-PD-L1 in one treatment. CCAZF + light plus anti-PD-L1 generated a great deal of CO under 650 nm laser irradiation, elevated ROS production in highly oxidatively stressed tumors by ICD, promoted inflammation and the release of tumor-associated antigens, effectively suppressed the formation of tumor nodules, and induced immune memory effects to
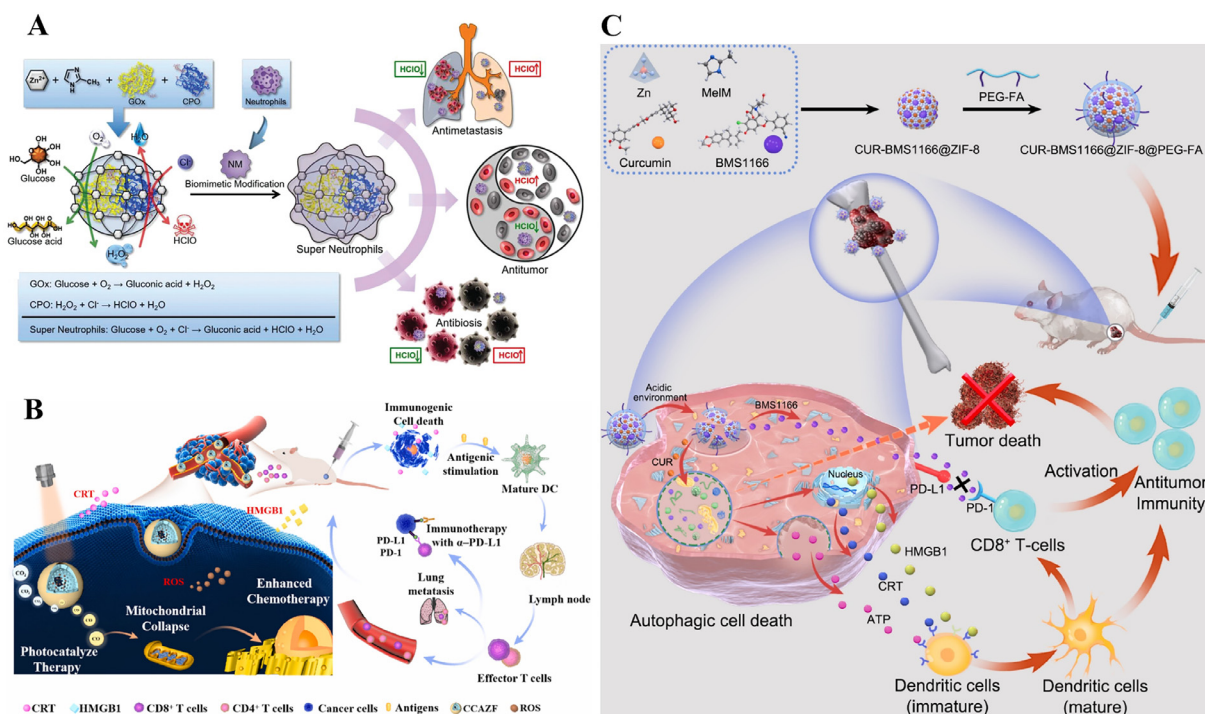
Fig. 7 – Schematic diagram of ZIF-based NPs for immunotherapy-based combination therapy. (A) Schematic of the biomimetic fabrication and mechanism of "super neutrophils." Reproduced from [162]. Copyright 2019 Wiley. (B) Schematic of the mechanisms of CCAZF with anti-PD-L1 for cancer immunotherapy. Reproduced from [163]. Copyright 2021 Elsevier. (C) Fabrication and therapeutic mechanism of CUR-BMS1166@ZIF-8@PEG-FA (CBZP). Reproduced from [189]. Copyright 2021 Elsevier.

inhibit the proliferation and metastasis of distal tumors [163] (Fig. 7B).

Ge and his coworkers designed an intelligent autophagy-controlling MOF, CUR-BMS1166@ZIF-8@PEG-FA (CBZP), to treat osteosarcoma effectively via autophagy-enhanced immunotherapy. The developed CBZP NPs contained the autophagy activator curcumin (CUR), an inhibitor of the PD-1/PD interaction BMS1166, which showed favorable biosafety and targeting ability, promoted ICD, blocked the immune checkpoint via autophagy, sensitized antitumor T-cell immunity, alleviated tumor immunogenicity deficiency, and achieved highly effective treatment of osteosarcoma [189] (Fig. 7C).

With in-depth research on ZIF nanomaterials, the mechanism by which ZIFs act on tumors has gradually been uncovered. Mn-Zn dual-ion release from ZIF-8@MnO2 combined with anti-PD-L1 antibody treatment effectively activates the cGAS-STING pathway and enhances the efficacy of immunotherapy, especially in p53-mutated tumors [190]. In addition, by loading aloe-emodin (AE) and coating ZIF-8 NPs with transferrin (Tf) and PEG-PLGA, AE@ZIF-8/Tf-PEG-PLGA NPs induced GBM tumor cell death by activating the CASP3/GSDME pyroptosis pathway [191]. Recent studies have shown that ZIF-8 NPs can induce cell death and activate the immune system, and synergistic treatment is more effective after being loaded with the mitochondrial depolarizing agent carbonyl cyanide m-chlorophenyl hydrazone (CCCP) [192]. This suggests that future studies need to pay more attention to the therapeutic advantages of ZIF NPs.

4.2.4. Other combination therapies

GOx can catalyze the conversion of glucose and O_2 to H_2O_2 and gluconic acid, decreasing the energy supply of tumors, and is widely used in starvation therapy and deoxygenation-activated chemotherapy of tumors [193]. Yu et al. constructed a ZIF nanoplatform (CHC/GOx@ZIF-8) for cooperative dual deprivation of lactate and glucose and enhancement of starvation therapy. In this study, the codelivery of the monocarboxylate transporter 1 inhibitor α-cyano-4-hydroxycinnamate (CHC) and GOx by ZIF-8 deprived the tumor of both lactate and glucose, blocked lactate-fueled respiration, relieved hypoxia in solid tumors, promoted the GOx catalytic activity of depleting extra glucose and produced more cytotoxic H_2O_2 to strengthen starvation therapy [194].

An ion interference-inductive starvation strategy was used for highly effective cancer therapy [94]. Wu et al. designed HZ@GD NPs in which HAase- and pH-sensitive ZIF-8 released superfluous Zn^{2+} that triggered nicotinamide adenine dinucleotide reduction and glyceraldehyde-phosphate dehydrogenase inactivation in cells to inhibit glycolysis. Moreover, the catalytic shearing of Zn^{2+}-activating GDs was activated only by Zn^{2+}, inhibited the expression of GLUT1, and decreased the glucose supply to achieve specific energy consumption in melanoma [94] (Fig. 8A). Chu et al. designed NIR-triggered UC-ZIF/berbamine (BER) NPs to regulate endogenous Ca^{2+} for cancer therapy. The UCNPs coated with nanosized ZIF-82 (UC-ZIF) released NO under NIR by isomerized nitro-nitrite in the ZIF-82 shell. NO combines with the overexpressed sulfhydryl group-rich
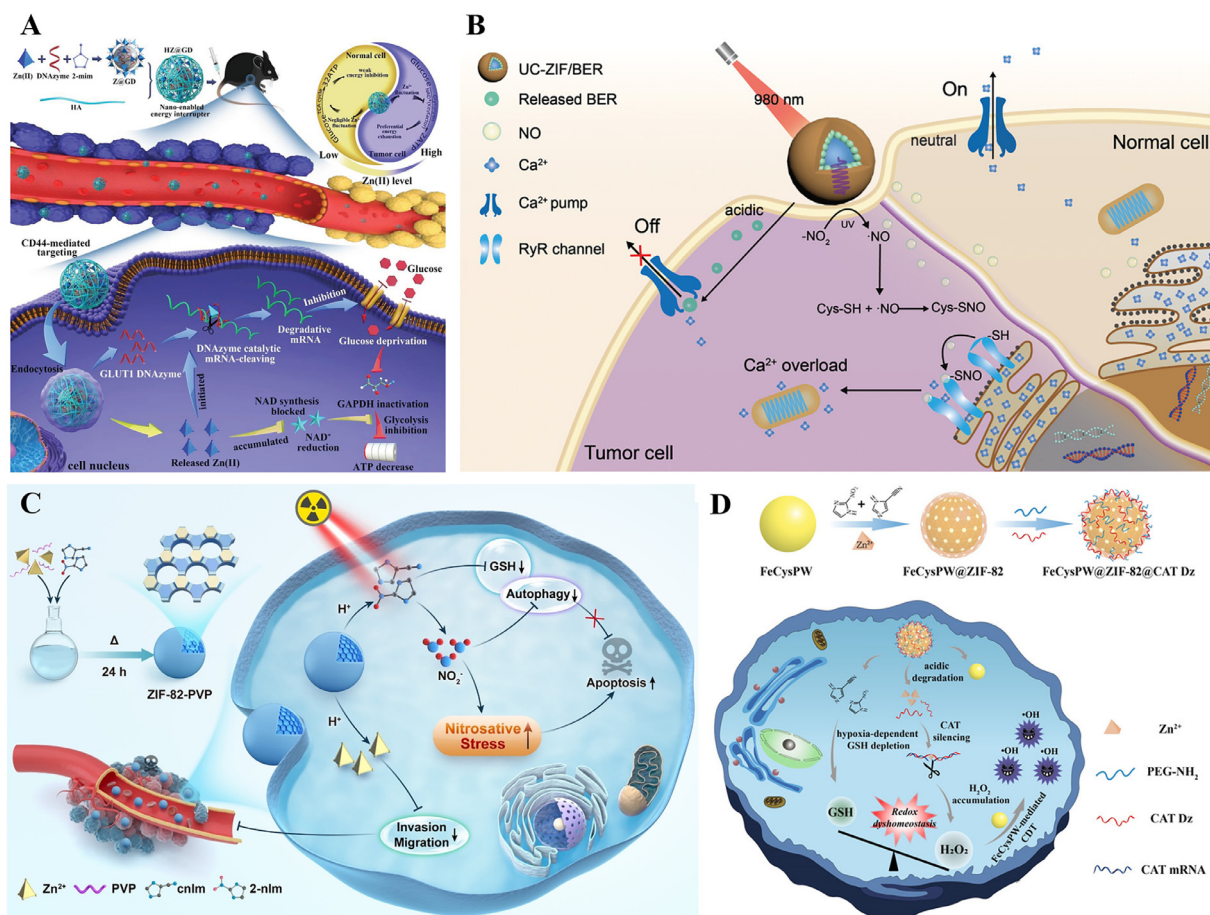
Fig. 8 – Schematic diagram of the use of ZIF-based NPs for metabolism-related combination therapy. (A) Schematic of the design and mechanism of a dual gate-controlled nanoenabled energy interrupter combined with Zn^{2+} involved in glycolysis inhibition with GLUT1 depletion in malignant melanoma. Reproduced from [94]. Copyright 2021 Wiley-VCH GmbH. (B) Schematic of the mechanism of UC-ZIF/BER in Ca^{2+}-initiated cancer therapy. Reproduced from [48]. Copyright 2021 Wiley. (C) Schematic of ZIF-82-PVP synthesis and the mechanisms of ZIF-82-PVP NPs in hypoxic prostate cancer therapy. Reproduced from [49]. Copyright 2021 Wiley. (D) Schematic illustration of the fabrication and multiple functions of FeCysPW@ZIF-82@CAT Dz. Reproduced from [50]. Copyright 2020 Wiley.

ryanodine receptor in the endoplasmic reticulum of tumor cells, undergoes protein S-nitrosylation, and then releases Ca^{2+}. NO and the calcium pump inhibitor BER in membranes maintain Ca^{2+} accumulation and inhibit Ca^{2+} efflux in tumor cells. Then, the induced ROS formation and effective overload of Ca^{2+} leads to cell death [48] (Fig. 8B).

Additionally, Li et al. synthesized ZIF-82-PVP NPs by a one-pot self-assembly method, which could disintegrate in an acidic TME. The dissociated Zn^{2+} specifically restrained the migration and invasion of prostate cancer cells. Moreover, the electrophilic 2-nIm ligand consumed GSH and produced NO_2^- upon X-ray irradiation in hypoxic cells. NO_2^- inhibited autophagy while enhancing lethal nitrosative stress levels to induce cell apoptosis in hypoxic tumors [49] (Fig. 8C). Based on the strategy of disrupting redox homeostasis in the TME, Li et al. synthesized pH/hypoxia/H_2O_2 stimuli-responsive FeCysPW@ZIF-82@CATDz NPs to kill hypoxic tumors [50]. ZIF-82 was assembled outside ferrous cysteine-phosphotungstate (FeCysPW), and then, CAT Dz was loaded

outside FeCysPW@ZIF-82 with the polymer mPEG-NH_2. CAT Dz-mediated mRNA silencing assisted by dissociated Zn^{2+} increased the intracellular H_2O_2 concentration. GSH depletion by electrophilic ZIF-82 under hypoxic conditions increased intracellular redox dyshomeostasis, reducing hypoxic tumor cell tolerance to ROS therapy, followed by FeCysPW converting H_2O_2 into ·OH and inducing CDT, which synergistically inhibited tumor growth (Fig. 8D).

Sonodynamic therapy (SDT) can trigger sonosensitizers to increase the concentration of ROS to kill tumor cells under ultrasound stimulation, with ultrasound penetrating deeper into the body than light [195]. Due to the stable performance of ZIFs under ultrasonic action, Liang et al. proposed a strategy for combining intraoperative hemostasis and postoperative sonodynamic therapy to prevent the recurrence of liver cancer [164] (Fig. 9A). Specifically, QCSG/HA-DA/ZDH (QH/ZDH) cryogels consisting of the hemostatic material glycidyl methacrylate-functionalized quaternized chitosan (QCSG), dopamine-HA, and the sonosensitizer hematoporphyrin
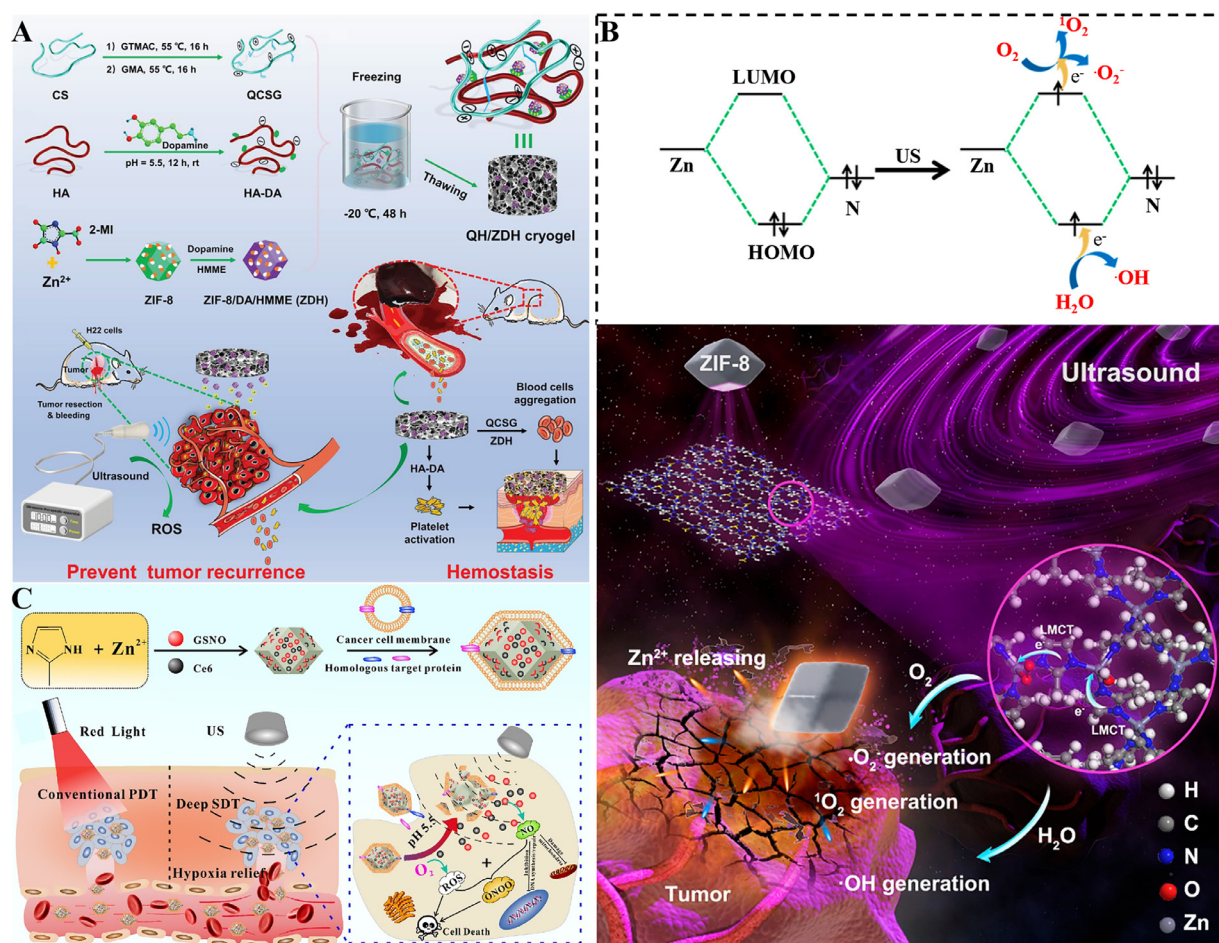
Fig. 9 – Schematic diagram of ZIF-based NPs for emerging combination therapy. (A) Schematic of the synthesis route of the QH/ZDH cryogel and its application in hemostasis and preventing tumor recurrence. Reproduced from [164]. Copyright 2021 Wiley. (B) Schematic of the use of ZIF-8 NCs for tumor therapy through combined bioactivity and sonodynamic properties. Reproduced from [55]. Copyright 2021 American Chemical Society. (C) Schematic of the fabrication of GCZ@M and gas-sonodynamic combined therapy. Reproduced from [165]. Copyright 2021 Elsevier.

monomethyl ether (HMME)-loaded dopamine-modified ZIF-8 (ZDH) were constructed, which recovered their shape via an intraoperative blood trigger and enhanced hemostasis, and also produced ROS by HMME under ultrasound and killed H22 cancer cells for postoperative prevention of tumor recurrence. In addition, the antibacterial property of Zn^{2+} reduced the potential for infection during surgery.

Recent studies have shown that as a bioactive anticancer agent and sonosensitizer under ultrasound irradiation, ZIF-8 nanocrystals with specific metal-nitrogen active sites exhibit high anticancer efficiency [55], which provides more directions and possibilities for the application of ZIF-8 in SDT (Fig. 9B). An et al. used ZIF-8 to encapsulate NO donors, nitro glutathione (GSNO), and the photosensitizer Ce6 together via coordination interactions between -COOH and Zn^{2+} to form a GSNO/Ce6@ZIF-8@Cytomembrane (GCZ@M) as a pH/ultrasound dual-response biomimetic nanoplatform. With the degradation of ZIF-8 in the acidic TME, ultrasound irradiation induced the decomposition of GSNO to NO and Ce6-mediated ROS generation. This nanoplatform enables a combination of nitric oxide and

sonodynamic therapy and repeatable ultrasound for relieving hypoxia [165] (Fig. 9C).

Radiotherapy (RT) or concurrent chemoradiotherapy (CCRT) plays an important role in cancer treatment [196]. Radiosensitization provides a new promising direction, and the combination of ZIF and radiation will provide a new way to enhance the effect of radiosensitization therapy in tumors [197]. FA-Mn_3O_4@ZIF-8 functions by targeting and stimulating responses to produce more $^1O_2$ under X-ray irradiation, alleviating hypoxia in the TME and promoting DNA damage and apoptosis in cervical cancer [198].

5.   Conclusion

As outlined above, ZIF-based nanomaterials have shown tremendous potential as smart materials with tunable responses (to pH, APT, ultrasound, $^1O_2$, hypoxia, UV, X-ray, etc.) for cancer treatment applications. The most popular ZIF-8 could be used as an anticancer agent and sonosensitizer, releasing Zn^{2+} to induce the apoptosis of tumor cells by

interrupting zinc homeostasis and degrading wide-spectrum mutant p53 proteins to treat cancer [55,120,190,199]. In addition to ZIF-8, ZIF-82 has shown significant promise in oncotherapy in the last two years, providing it with more tunable functionalities because of its organic ligands. ZIF-based nanomaterials have the properties of maintaining the biological activity of biomacromolecules, protecting them from the effects of the environment and realizing controllable release in response to specific triggers.

ZIF-based nanomaterials suffer from many ongoing challenges and limitations in cancer therapy that need to be addressed, mainly in terms of toxicity in cell proliferation and metabolism. The ions, organic bridging ligands, and organic solvents could show toxicity *in vivo*. ZIFs may disassemble into other poisonous degradation products or metabolites, causing mitochondrial and lysosomal dysfunction. Free Zn^{2+} cations might compete with Fe^{2+} and Ca^{2+} cations, causing transcriptional regulation, protein synthesis, and DNA damage dysfunctions [200,201]. An increase in intracellular Zn^{2+} leads to ROS generation and cellular inflammation, which induces a pause in the G2/M phase of the cell cycle and leads to cell apoptosis [201–203]. The elevated Zn^{2+} released from low doses of ZIF-8 NPs directly disrupted actin polymerization and caused structural alterations, such as in the branching and contractility of vascular smooth muscle cells [204], increasing the risk of cardiovascular disease.

From the cell morphology perspective, 12.5 µg/ml was the minimum toxic concentration, while from the cell viability perspective, a ZIF-8 NP concentration of 25 µg/ml was deemed "safe" by conventional biochemical cell assays [204]. At concentrations <30 µg/ml, ZIF-8 had no significant cytotoxicity on various body parts, such as the kidney, skin, breast, blood, bones, or connective tissue [201]. A concentration of ZIF-8 above the critical threshold (over 30 µg/ml) resulted in a concentration-dependent increase in ROS and irreversible DNA damage in cells, significantly reduced biocompatibility characteristics, possibly caused cell membrane damage [204], and decreased cell viability significantly.

ZIF-8 was proven to be hematocompatible, while ZIF-67 bound to hemoglobin via electrostatic interactions, changed the microenvironment and structure of hemoglobin, inhibited the oxygen-carrying ability and release of heme from hemoglobin, and caused significant hemolysis [205]. In addition to the toxicity of residual solvents or additives in ZIFs, the chemical composition, dosage, size, colloidal and chemical stability, and route of administration/exposure of ZIF-based nanomaterials [206] can all cause toxicity in human tissues. Drug metabolism in the body is a complex process compared to studies at the cellular level.

In experiments on zebrafish embryos and adult fish treated with the MG@ZIF-L nanocomposite, no significant deformities were observed at the highest dose of 200 µg/ml [207]. After treatment with lanthanide-doped NPs@Fe/Mn-ZIF-8, the routine blood parameters, liver and kidney function parameters and morphology of important organs of tumor-bearing mice did not significantly change, and their survival time significantly improved compared with that of other groups [208]. Pathological changes in the liver and kidney and partial liver function abnormalities were observed after intravenous injection of 5-Fu@ZIF-NPs (32 mg/kg) in an ICR mouse model [123]. After intranasal infusion of nanoscale ZIF-67 at a nontoxic dose for 30 d, rats showed neurotoxic effects of ZIF-67 and exhibited impaired spatial learning and memory in neurobehavioral experiments [209].

Therefore, further research is needed to explore the appropriate concentration and modifications of ZIFs and solve the toxic effects of ZIFs on cells and tissues. In brief, the short- and long-term metabolism and toxicity of ZIF-based NPs need to be considered. The appropriate modification of ZIF-based NPs and combination therapy to reduce the applied dose of toxic drugs are meaningful.

Despite cell membranes and polymers being modified on ZIFs, NP platforms still require further optimized surface functionalization and assessment of *in vivo* toxicity profiles before being implemented clinically. ZIF-based oncotherapy has reached the animal testing stage. 3D cancer models and patient-derived xenograft (PDX) models could compensate for the inadequate representation of physiological complexity in two-dimensional (2D) cell cultures and mimic the TME and nutrient supply, increasing the reliability of the anticancer effectiveness of DDSs [210]. Many articles have shown the short-term biosecurity of ZIF-based nanomaterials by testing biochemical reactions [183,170]. The single-cell level biosafety, long-term biosafety, and comprehensive understanding of the mechanism of absorption-distribution-metabolism-excretion of ZIFs remain to be studied.

Based on the properties of ZIF nanomaterials, treatment can also be combined with diagnostic [211], imaging [151], catalytic [163] and sensing [19] modalities to synergistically understand the progress of diagnosis and treatment, thereby enhancing therapeutic efficacy. In addition, the antitumor efficacy, preparation method, and economic benefit of ZIF nanomaterials should be considered, as well as the feasibility of clinical transformation, instead of simply pursuing complex treatment methods and carrying too many materials. It is hoped that safe, sustainable, and highly biocompatible green synthetic ZIF-based nanocomposites can be obtained through reasonable design under multidisciplinary efforts. ZIF-based nanocomposites are expected to flourish, achieve accurate and efficient treatment of tumors, and be applied in the clinic early.

Conflicts of interest

The authors report no conflicts of interest. The authors alone are responsible for the content and writing of this article.

Acknowledgements

References

[1] Siegel RL, Miller KD, Fuchs HE, Jemal A. Cancer statistics, 2021. CA Cancer J. Clin 2021;71:7–33.

[2] GlobalSurg Collaborative and National Institute for Health Research Global Health Research Unit on Global SurgeryGlobal variation in postoperative mortality and complications after cancer surgery: a multicentre, prospective cohort study in 82 countries. Lancet 2021;397:387–97.

[3] Wang J, Zhu M, Nie G. Biomembrane-based nanostructures for cancer targeting and therapy: from synthetic liposomes to natural biomembranes and membrane-vesicles. Adv Drug Deliv Rev 2021;178:113974.

[4] Chung S, Revia RA, Zhang M. Graphene quantum dots and their applications in bioimaging, biosensing, and therapy. Adv Mater 2021;33:e1904362.

[5] Živojević K, Mladenović M, Djisalov M, Mundzic M, Ruiz-Hernandez E, Gadjanski I, et al. Advanced mesoporous silica nanocarriers in cancer theranostics and gene editing applications. J Control Release 2021;337:193–211.

[6] Wang S, Liu X, Yang M, Ouyang L, Ding J, Wang S, et al. Non-cytotoxic nanoparticles re-educating macrophages achieving both innate and adaptive immune responses for tumor therapy. Asian J Pharm 2022;17:557–70.

[7] Wang C, Wang J, Pan X, Yu S, Chen M, Gao Y, et al. Reversing ferroptosis resistance by MOFs through regulation intracellular redox homeostasis. Asian J Pharm 2023;18:100770.

[8] Medici S, Peana M, Coradduzza D, Zoroddu MA. Gold nanoparticles and cancer: detection, diagnosis and therapy. Semin Cancer Biol 2021;76:27–37.

[9] Wuttke S, Lismont M, Escudero A, Rungtaweevoranit B, Parak WJ. Positioning metal-organic framework nanoparticles within the context of drug delivery – a comparison with mesoporous silica nanoparticles and dendrimers. Biomaterials 2017;123:172–83.

[10] Mallakpour S, Nikkhoo E, Hussain CM. Application of MOF materials as drug delivery systems for cancer therapy and dermal treatment. Coord Chem Rev 2022;451:214262.

[11] Banerjee R, Phan A, Wang B, Knobler C, Furukawa H, O'Keeffe M, et al. High-throughput synthesis of zeolitic imidazolate frameworks and application to CO_2 Capture. Science 2008;319:939–43.

[12] James JB, Lin YS. Kinetics of ZIF-8 thermal decomposition in inert, oxidizing, and reducing environments. J Phys Chem C 2016;120:14015–26.

[13] Ding Y, Xu Y, Yang W, Niu P, Li X, Chen Y, et al. Investigating the EPR effect of nanomedicines in human renal tumors via *ex vivo* perfusion strategy. Nano Today 2020;35:100970.

[14] Ren SZ, Wang B, Zhu XH, Zhu D, Liu M, Li SK, et al. Oxygen self-sufficient core-shell metal-organic framework-based smart nanoplatform for enhanced synergistic chemotherapy and photodynamic therapy. ACS Appl Mater Interfaces 2020;12:24662–74.

[15] Deng J, Wang K, Wang M, Yu P, Mao L. Mitochondria targeted nanoscale zeolitic imidazole framework-90 for ATP imaging in live cells. J Am Chem Soc 2017;139:5877–82.

[16] Li PZ, Aranishi K, Xu Q. ZIF-8 immobilized nickel nanoparticles: highly effective catalysts for hydrogen generation from hydrolysis of ammonia borane. Chem Commun 2012;48:3173–5.

[17] Budi CS, Deka JR, Hsu WC, Saikia D, Chen KT, Kao HM, et al. Bimetallic Co/Zn zeolitic imidazolate framework ZIF-67 supported Cu nanoparticles: an excellent catalyst for reduction of synthetic dyes and nitroarenes. J Hazard Mater 2021;407:124392.

[18] Ma X, Wan Z, Li Y, He X, Caro J, Huang A. Anisotropic gas separation in oriented ZIF-95 membranes prepared by vapor-assisted in-plane epitaxial growth. Angew Chem Int Ed Engl 2020;59:20858–62.

[19] Kong L, Lv S, Qiao Z, Yan Y, Zhang J, Bi S. Metal-organic framework nanoreactor-based electrochemical biosensor coupled with three-dimensional DNA walker for label-free detection of microRNA. Biosens Bioelectron 2022;207:114188.

[20] Chen WH, Luo GF, Vázquez-González M, Cazelles R, Sohn YS, Nechushtai R, et al. Glucose-responsive metal-organic-framework nanoparticles act as "smart" sense-and-treat carriers. ACS Nano 2018;12:7538–45.

[21] Zhu X, Xu J, Ling G, Zhang P. Tunable metal–organic frameworks assist in catalyzing DNAzymes with amplification platforms for biomedical applications. Chem Soc Rev 2023;52:7549–78.

[22] Zeng Y, Liao D, Kong X, Huang Q, Zhong M, Liu J, et al. Current status and prospect of ZIF-based materials for breast cancer treatment. Colloids Surf B 2023;232:113612.

[23] Ge X, Wong R, Anisa A, Ma S. Recent development of metal-organic framework nanocomposites for biomedical applications. Biomaterials 2021;281:121322.

[24] Park KS, Ni Z, Côté AP, Choi JY, Huang R, Uribe-Romo FJ, et al. Exceptional chemical and thermal stability of zeolitic imidazolate frameworks. Proc Natl Acad Sci U S A 2006;103:10186–91.

[25] Shen J, Ma M, Shafiq M, Yu H, Lan Z, Chen H. Microfluidics-assisted engineering of pH/enzyme dual-activatable ZIF@polymer nanosystem for co-delivery of proteins and chemotherapeutics with enhanced deep-tumor penetration. Angew Chem Int Ed Engl 2022:e202113703.

[26] Li R, Ren X, Zhao J, Feng X, Jiang X, Fan X, et al. Polyoxometallates trapped in a zeolitic imidazolate framework leading to high uptake and selectivity of bioactive molecules. J Mater Chem A 2014;2:2168–73.

[27] Wei Y, Chang M, Liu J, Wang N, Wang JX. Spray drying-assisted construction of hierarchically porous ZIF-8 for controlled release of doxorubicin. Nanoscale 2022;14:2793–801.

[28] Sun CY, Qin C, Wang XL, Yang GS, Shao KZ, Lan YQ, et al. Zeolitic imidazolate framework-8 as efficient pH-sensitive drug delivery vehicle. Dalton Trans 2012;41:6906–9.

[29] Zheng H, Zhang Y, Liu L, Wan W, Guo P, Nyström AM, et al. One-pot synthesis of metal-organic frameworks with encapsulated target molecules and their applications for controlled drug delivery. J Am Chem Soc 2016;138:962–8.

[30] Qiu J, Tomeh MA, Jin Y, Zhang B, Zhao X. Microfluidic formulation of anticancer peptide loaded ZIF-8 nanoparticles for the treatment of breast cancer. J. Colloid Interface Sci 2023;642:810–19.

[31] Zhang H, Hao C, Qu A, Sun M, Xu L, Xu C, et al. Heterostructures of MOFs and nanorods for multimodal imaging. Adv Funct Mater 2018;28:1805320.

[32] Balachandran YL, Li X, Jiang X. Integrated microfluidic synthesis of aptamer functionalized biozeolitic imidazolate framework (BioZIF-8) targeting lymph node and tumor. Nano Lett 2021;21:1335–44.

[33] Siboro PY, Nguyen VKT, Miao YB, Sharma AK, Mi FL, Chen HL, et al. Ultrasound-activated, tumor-specific *in situ* synthesis of a chemotherapeutic agent using ZIF-8 nanoreactors for precision cancer therapy. ACS Nano 2022;16:12403–14.

[34] Riley CM, Sternson LA. In: Florey K, editor. Analytical profiles of drug substances, 14. New York: Academic Press; 1985. p. 77–105.

[35] Zieske PA, Koberda M, Hines JL, Knight CC, Sriram R, Raghavan NV, et al. Characterization of cisplatin degradation as affected by pH and light. Am J Hosp Pharm 1991;48:1500–6.

[36] Xing Y, Jiang Z, Akakuru OU, He Y, Li A, Li J, et al. Mitochondria-targeting zeolitic imidazole frameworks to overcome platinum-resistant ovarian cancer. Colloids Surf B 2020;189:110837.

[37] Jin CX, Shang HB. Synthetic methods, properties and controlling roles of synthetic parameters of zeolite imidazole framework-8: a review. J Solid State Chem 2021;297:122040.

[38] Zakhia Douaihy R, Al-Ghoul M, Hmadeh M. Liesegang banding for controlled size and growth of zeolitic-imidazolate frameworks. Small 2019;15:e1901605.

[39] Cravillon J, Münzer S, Lohmeier SJ, Feldhoff A, Huber K, Wiebcke M. Rapid room-temperature synthesis and characterization of nanocrystals of a prototypical zeolitic imidazolate framework. Chem Mater 2009;21:1410–12.

[40] Venna SR, Jasinski JB, Carreon MA. Structural evolution of zeolitic imidazolate framework-8. J Am Chem Soc 2010;132:18030–3.

[41] Ryu U, Jee S, Rao PC, Shin J, Ko C, Yoon M, et al. Recent advances in process engineering and upcoming applications of metal–organic frameworks. Coord Chem Rev 2021;426:213544.

[42] Tsai CW, Langner EHG. The effect of synthesis temperature on the particle size of nano-ZIF-8. Microporous Mesoporous Mater 2016;221:8–13.

[43] Zhang Y, Jia Y, Li M, Hou L. Influence of the 2-methylimidazole/zinc nitrate hexahydrate molar ratio on the synthesis of zeolitic imidazolate framework-8 crystals at room temperature. Sci Rep 2018;8:9597.

[44] Sa M, Td B, Ak C. The effect of pressure on ZIF-8: increasing pore size with pressure and the formation of a high-pressure phase at 1.47 GPa. Angew Chem Int Ed Engl 2009;48.

[45] Zhuang J, Kuo CH, Chou LY, Liu DY, Weerapana E, Tsung CK. Optimized metal-organic-framework nanospheres for drug delivery: evaluation of small-molecule encapsulation. ACS Nano 2014;8:2812–19.

[46] Howarth AJ, Liu Y, Li P, Li Z, Wang TC, Hupp JT, et al. Chemical, thermal and mechanical stabilities of metal–organic frameworks. Nat Rev Mater 2016;1:1–15.

[47] Li X, Gao M, Xin K, Zhang L, Ding D, Kong D, et al. Singlet oxygen-responsive micelles for enhanced photodynamic therapy. J Control Release 2017;260:12–21.

[48] Chu X, Jiang X, Liu Y, Zhai S, Jiang Y, Chen Y, et al. Nitric oxide modulating calcium store for Ca^{2+}-initiated cancer therapy. Adv Funct Mater 2021;31:2008507.

[49] Li Y, Gong T, Gao H, Chen Y, Li H, Zhao P, et al. ZIF-based nanoparticles combine X-ray-induced nitrosative stress with autophagy management for hypoxic prostate cancer therapy. Angew Chem Int Ed 2021;60:15472–81.

[50] Li Y, Zhao P, Gong T, Wang H, Jiang X, Cheng H, et al. Redox dyshomeostasis strategy for hypoxic tumor therapy based on DNAzyme-loaded electrophilic ZIFs. Angew Chem Int Ed 2020;59:22537–43.

[51] Gomar M, Yeganegi S. Adsorption of 5-fluorouracil, hydroxyurea and mercaptopurine drugs on zeolitic imidazolate frameworks (ZIF-7, ZIF-8 and ZIF-9). Microporous Mesoporous Mater 2017;252:167–72.

[52] Thompson MJ, Wells SA, Düren T. Cisplatin uptake and release in pH sensitive zeolitic imidazole frameworks. J Chem Phys 2021;154:244703.

[53] Cao Y, Jiang Z, Li Y, Wang Y, Yang Y, Akakuru OU, et al. Tandem post-synthetic modification of a zeolitic imidazolate framework for CXCR4-overexpressed esophageal squamous cell cancer imaging and therapy. Nanoscale 2020;12:12779–89.

[54] Kukkar P, Kim K-H, Kukkar D, Singh P. Recent advances in the synthesis techniques for zeolitic imidazolate frameworks and their sensing applications. Coord Chem Rev 2021;446:214109.

[55] Wang W, Pan X, Yang H, Wang H, Wu Q, Zheng L, et al. Bioactive metal-organic frameworks with specific metal-nitrogen (M-N) active sites for efficient sonodynamic tumor therapy. ACS Nano 2021;15:20003–12.

[56] Wu J, Zhang Z, Qiao C, Yi C, Xu Z, Chen T, et al. Synthesis of monodisperse ZIF-67@CuSe@PVP nanoparticles for pH-responsive drug release and photothermal therapy. ACS Biomater Sci Eng 2022;8:284–92.

[57] Gao S, Jin Y, Ge K, Li Z, Liu H, Dai X, et al. Self-supply of O_2 and H_2O_2 by a nanocatalytic medicine to enhance combined chemo/chemodynamic therapy. Adv Sci 2019;6:1902137.

[58] Jiang Z, Wang Y, Sun L, Yuan B, Tian Y, Xiang L, et al. Dual ATP and pH responsive ZIF-90 nanosystem with favorable biocompatibility and facile post-modification improves therapeutic outcomes of triple negative breast cancer *in vivo*. Biomaterials 2019;197:41–50.

[59] Meng X, Jia K, Sun K, Zhang L, Wang Z. Smart responsive nanoplatform via *in situ* forming disulfiram-copper ion chelation complex for cancer combination chemotherapy. Chem Eng J 2021;415:128947.

[60] Zheng M, Liu S, Guan X, Xie Z. One-step synthesis of nanoscale zeolitic imidazolate frameworks with high curcumin loading for treatment of cervical cancer. ACS Appl Mater Interfaces 2015;7:22181–7.

[61] Jiang Z, Li Y, Wei Z, Yuan B, Wang Y, Akakuru OU, et al. Pressure-induced amorphous zeolitic imidazole frameworks with reduced toxicity and increased tumor accumulation improves therapeutic efficacy *in vivo*. Bioact Mater 2021;6:740–8.

[62] Liédana N, Galve A, Rubio C, Téllez C, Coronas J. CAF@ZIF-8: one-step encapsulation of caffeine in MOF. ACS Appl Mater Interfaces 2012;4:5016–21.

[63] Mohammadinejad R, Moosavi MA, Tavakol S, Vardar DÖ, Hosseini A, Rahmati M, et al. Necrotic, apoptotic and autophagic cell fates triggered by nanoparticles. Autophagy 2019;15:4–33.

[64] Zhang S, Li J, Lykotrafitis G, Bao G, Suresh S. Size-dependent endocytosis of nanoparticles. Adv Mater 2009;21:419–424.

[65] Yu Q, Tian Y, Li M, Jiang Y, Sun H, Zhang G, et al. Poly(ethylene glycol)-mediated mineralization of metal-organic frameworks. Chem Commun 2020;56:11078–81.

[66] Zhou X, Zhou A, Tian Z, Chen W, Xu Y, Ning X, et al. A responsive nanorobot modulates intracellular zinc homeostasis to amplify mitochondria-targeted phototherapy. Small 2023;19:2302952.

[67] Wang B, Su X, Liang J, Yang L, Hu Q, Shan X, et al. Synthesis of polymer-functionalized nanoscale graphene oxide with different surface charge and its cellular uptake, biosafety and immune responses in Raw264.7 macrophages. Mater Sci Eng. C 2018;90:514–22.

[68] Mu J, He L, Huang P, Chen X. Engineering of nanoscale coordination polymers with biomolecules for advanced applications. Coord Chem Rev 2019;399:213039.

[69] Liu X, Huang N, Wang H, Li H, Jin Q, Ji J. The effect of ligand composition on the *in vivo* fate of multidentate poly(ethylene glycol) modified gold nanoparticles. Biomaterials 2013;34:8370–81.

[70] Shi Z, Chen X, Zhang L, Ding S, Wang X, Lei Q, et al. FA-PEG decorated MOF nanoparticles as a targeted drug delivery system for controlled release of an autophagy inhibitor. Biomater Sci 2018;6:2582–90.

[71] Soo Choi H, Liu W, Misra P, Tanaka E, Zimmer JP, Itty Ipe B, et al. Renal clearance of quantum dots. Nat Biotechnol 2007;25:1165–70.

[72] Wang H, Li T, Li J, Tong W, Gao C. One-pot synthesis of poly(ethylene glycol) modified zeolitic imidazolate framework-8 nanoparticles: size control, surface

modification and drug encapsulation. Colloids Surf A Physicochem Eng Asp 2019;568:224–30.

[73] Kozma GT, Shimizu T, Ishida T, Szebeni J. Anti-PEG antibodies: properties, formation, testing and role in adverse immune reactions to PEGylated nano-biopharmaceuticals. Adv Drug Deliv Rev 2020;154–155:163–75.

[74] Gabizon A, Szebeni J. Complement activation: a potential threat on the safety of poly(ethylene glycol)-coated nanomedicines. ACS Nano 2020;14:7682–8.

[75] Lu G, Li S, Guo Z, Farha OK, Hauser BG, Qi X, et al. Imparting functionality to a metal-organic framework material by controlled nanoparticle encapsulation. Nature Chem 2012;4:310–16.

[76] Wu Q, Niu M, Chen X, Tan L, Fu C, Ren X, et al. Biocompatible and biodegradable zeolitic imidazolate framework/polydopamine nanocarriers for dual stimulus triggered tumor thermo-chemotherapy. Biomaterials 2018;162:132–43.

[77] Liu F, Lin L, Zhang Y, Sheng S, Wang Y, Xu C, et al. Two-dimensional nanosheets with high curcumin loading content for multimodal imaging-guided combined chemo-photothermal therapy. Biomaterials 2019;223:119470.

[78] Li Y, Zhang K, Liu P, Chen M, Zhong Y, Ye Q, et al. Encapsulation of plasmid DNA by nanoscale metal-organic frameworks for efficient gene transportation and expression. Adv Mater 2019;31:e1901570.

[79] Jennings JA, Wells CM, McGraw GS, Velasquez Pulgarin DA, Whitaker MD, Pruitt RL, et al. Chitosan coatings to control release and target tissues for therapeutic delivery. Ther Deliv 2015;6:855–71.

[80] Faraji Dizaji B, Hasani Azerbaijan M, Sheisi N, Goleij P, Mirmajidi T, Chogan F, et al. Synthesis of PLGA/chitosan/zeolites and PLGA/chitosan/metal organic frameworks nanofibers for targeted delivery of paclitaxel toward prostate cancer cells death. Int J Biol Macromol 2020;164:1461–74.

[81] Guidotti G, Brambilla L, Rossi D. Cell-penetrating peptides: from basic research to clinics. Trends Pharmacol 2017;38:406–24.

[82] Abdelhamid HN, Dowaidar M, Hällbrink M, Langel Ü. Gene delivery using cell penetrating peptides-zeolitic imidazolate frameworks. Microporous and Mesoporous Mater 2020;300:110173.

[83] Fu X, Zhang G, Zhang Y, Sun H, Yang S, Ni S, et al. Co-delivery of anticancer drugs and cell penetrating peptides for improved cancer therapy. Chin Chem Lett 2021;32:1559–1562.

[84] Temming K, Schiffelers RM, Molema G, Kok RJ. RGD-based strategies for selective delivery of therapeutics and imaging agents to the tumour vasculature. Drug Resist Updat 2005;8:381–402.

[85] Dong K, Zhang Y, Zhang L, Wang Z, Ren J, Qu X. Facile preparation of metal-organic frameworks-based hydrophobic anticancer drug delivery nanoplatform for targeted and enhanced cancer treatment. Talanta 2019;194:703–8.

[86] Lin Y, Zhong Y, Chen Y, Li L, Chen G, Zhang J, et al. Ligand-modified erythrocyte membrane-cloaked metal-organic framework nanoparticles for targeted antitumor therapy. Mol Pharm 2020;17:3328–41.

[87] Dalle Vedove E, Costabile G, Merkel OM. Mannose and mannose-6-phosphate receptor–targeted drug delivery systems and their application in cancer therapy. Adv Healthc Mater 2018;7:1701398.

[88] Zhang H, Zhang J, Li Q, Song A, Tian H, Wang J, et al. Site-specific MOF-based immunotherapeutic nanoplatforms via synergistic tumor cells-targeted treatment and dendritic cells-targeted immunomodulation. Biomaterials 2020;245:119983.

[89] Zhang Y, Zheng DW, Li CX, Pan P, Zeng SM, Pan T, et al. Temulence therapy to orthotopic colorectal tumor via oral administration of fungi-based acetaldehyde generator. Small Methods 2022;6:2100951.

[90] Liang J, Jiang D, Noble PW. Hyaluronan as a therapeutic target in human diseases. Adv Drug Deliv Rev 2016;97:186–203.

[91] Gao Y, Foster R, Yang X, Feng Y, Shen JK, Mankin HJ, et al. Up-regulation of CD44 in the development of metastasis, recurrence and drug resistance of ovarian cancer. Oncotarget 2015;6:9313–26.

[92] Chen C, Zhao S, Karnad A, Freeman JW. The biology and role of CD44 in cancer progression: therapeutic implications. J Hematol Oncol 2018;11:64.

[93] Liu X, Taftaf R, Kawaguchi M, Chang YF, Chen W, Entenberg D, et al. Homophilic CD44 interactions mediate tumor cell aggregation and polyclonal metastasis in patient-derived breast cancer models. Cancer Discov 2019;9:96–113.

[94] Wu S, Zhang K, Liang Y, Wei Y, An J, Wang Y, et al. Nano-enabled tumor systematic energy exhaustion via zinc (II) interference mediated glycolysis inhibition and specific GLUT1 depletion. Adv Sci 2021:2103534.

[95] Sun Q, Bi H, Wang Z, Li C, Wang X, Xu J, et al. Hyaluronic acid-targeted and pH-responsive drug delivery system based on metal-organic frameworks for efficient antitumor therapy. Biomaterials 2019;223:119473.

[96] Elnakat H, Ratnam M. Distribution, functionality and gene regulation of folate receptor isoforms: implications in targeted therapy. Adv Drug Deliv Rev 2004;56:1067–84.

[97] Qin YT, Peng H, He XW, Li WY, Zhang YK. pH-responsive polymer-stabilized ZIF-8 nanocomposites for fluorescence and magnetic resonance dual-modal imaging-guided chemo-/photodynamic combinational cancer therapy. ACS Appl Mater Interfaces 2019;11:34268–81.

[98] Zhou Y, Cao HB, Li WJ, Zhao L. The CXCL12 (SDF-1)/CXCR4 chemokine axis: oncogenic properties, molecular targeting, and synthetic and natural product CXCR4 inhibitors for cancer therapy. Chin J Nat Med 2018;16:801–10.

[99] Zhang L, Bijker MS, Herzog H. The neuropeptide Y system: pathophysiological and therapeutic implications in obesity and cancer. Pharmacol Ther 2011;131:91–113.

[100] Hofmann S, Bellmann-Sickert K, Beck-Sickinger AG. Chemical modification of neuropeptide Y for human Y1 receptor targeting in health and disease. Biol Chem 2019;400:299–311.

[101] Böhme D, Krieghoff J, Beck-Sickinger AG. Double methotrexate-modified neuropeptide Y analogues express increased toxicity and overcome drug resistance in breast cancer cells. J Med Chem 2016;59:3409–17.

[102] Jiang Z, Yuan B, Qiu N, Wang Y, Sun L, Wei Z, et al. Manganese-zeolitic imidazolate frameworks-90 with high blood circulation stability for MRI-guided tumor therapy. Nano-Micro Lett 2019;11:61.

[103] Zhu G, Chen X. Aptamer-based targeted therapy. Adv Drug Deliv Rev 2018;134:65–78.

[104] Bamrungsap S, Treetong A, Apiwat C, Wuttikhun T, Dharakul T. SERS-fluorescence dual mode nanotags for cervical cancer detection using aptamers conjugated to gold-silver nanorods. Microchim Acta 2016;183:249–56.

[105] Feng J, Xu Z, Dong P, Yu W, Liu F, Jiang Q, et al. Stimuli-responsive multifunctional metal–organic framework nanoparticles for enhanced chemo-photothermal therapy. J Mater Chem B 2019;7:994–1004.

[106] Dong K, Wang Z, Zhang Y, Ren J, Qu X. Metal-organic framework-based nanoplatform for intracellular environment-responsive endo/lysosomal escape and

enhanced cancer therapy. ACS Appl Mater Interfaces 2018;10:31998–2005.

[107] Lu L, Liu G, Lin C, Li K, He T, Zhang J, et al. Mitochondrial metabolism targeted nanoplatform for efficient triple-negative breast cancer combination therapy. Adv Healthc Mater 2021;10:2100978.

[108] Chen HY, Deng J, Wang Y, Wu CQ, Li X, Dai HW. Hybrid cell membrane-coated nanoparticles: a multifunctional biomimetic platform for cancer diagnosis and therapy. Acta Biomater 2020;112:1–13.

[109] Subramanian S, Parthasarathy R, Sen S, Boder ET, Discher DE. Species- and cell type-specific interactions between CD47 and human SIRPα. Blood 2006;107:2548–56.

[110] Xia Q, Zhang Y, Li Z, Hou X, Feng N. Red blood cell membrane-camouflaged nanoparticles: a novel drug delivery system for antitumor application. Acta Pharm Sin B 2019;9:675–89.

[111] Lublin DM, Atkinson JP. Decay-accelerating factor: biochemistry, Molecular Biology, and Function. Annu Rev Immunol 1989;7:35–58.

[112] Zhang L, Wang Z, Zhang Y, Cao F, Dong K, Ren J, et al. Erythrocyte membrane cloaked metal-organic framework nanoparticle as biomimetic nanoreactor for starvation-activated colon cancer therapy. ACS Nano 2018;12:10201–11.

[113] Qiao C, Wang X, Liu G, Yang Z, Jia Q, Wang L, et al. Erythrocyte membrane camouflaged metal-organic framework nanodrugs for remodeled tumor microenvironment and enhanced tumor chemotherapy. Adv Funct Mater 2022;32:2107791.

[114] Zhang Y, Yang L, Wang H, Huang J, Lin Y, Chen S, et al. Bioinspired metal-organic frameworks mediated efficient delivery of siRNA for cancer therapy. Chem Eng J 2021;426:131926.

[115] Shao F, Wu Y, Tian Z, Liu S. Biomimetic nanoreactor for targeted cancer starvation therapy and cascade amplified chemotherapy. Biomaterials 2021;274:120869.

[116] Zou MZ, Liu WL, Li CX, Zheng DW, Zeng JY, Gao F, et al. A multifunctional biomimetic nanoplatform for relieving hypoxia to enhance chemotherapy and inhibit the PD-1/PD-L1 axis. Small 2018;14:e1801120.

[117] Gao C, Lin Z, Jurado-Sánchez B, Lin X, Wu Z, He Q. Stem cell membrane-coated nanogels for highly efficient *in vivo* tumor targeted drug delivery. Small 2016;12:4056–62.

[118] Liang N, Ren N, Feng Z, Sun Z, Dong M, Wang W, et al. Biomimetic metal-organic frameworks as targeted vehicles to enhance osteogenesis. Adv Healthc Mater 2022;11:2102821.

[119] Liao Y, Zhang Y, Blum NT, Lin J, Huang P. Biomimetic hybrid membrane-based nanoplatforms: synthesis, properties and biomedical applications. Nanoscale Horiz 2020;5:1293–302.

[120] Zhang Y, Huang X, Wang L, Cao C, Zhang H, Wei P, et al. Glutathionylation-dependent proteasomal degradation of wide-spectrum mutant p53 proteins by engineered zeolitic imidazolate framework-8. Biomaterials 2021;271:120720.

[121] Zhou X, Zhao W, Wang M, Zhang S, Li Y, Hu W, et al. Dual-modal therapeutic role of the lactate oxidase-embedded hierarchical porous zeolitic imidazolate framework as a nanocatalyst for effective tumor suppression. ACS Appl Mater Interfaces 2020;12:32278–88.

[122] Yang B, Chen Y, Shi J. Reactive oxygen species (ROS)-based nanomedicine. Chem Rev 2019;119:4881–985.

[123] Li S, Wang K, Shi Y, Cui Y, Chen B, He B, et al. Novel biological functions of ZIF-NP as a delivery vehicle: high pulmonary accumulation, favorable biocompatibility, and improved therapeutic outcome. Adv Funct Mater 2016;26:2715–27.

[124] Samiei Foroushani M, Zahmatkeshan A, Arkaban H, Karimi Shervedani R, Kefayat A. A drug delivery system based on nanocomposites constructed from metal-organic frameworks and Mn_3O_4 nanoparticles: preparation and physicochemical characterization for BT-474 and MCF-7 cancer cells. Colloids Surf B Biointerfaces 2021;202:111712.

[125] Abd Al-Jabbar S, Atiroğlu V, Hameed RM, Guney Eskiler G, Atiroğlu A, Deveci Ozkan A, et al. Fabrication of dopamine conjugated with protein @metal organic framework for targeted drug delivery: a biocompatible pH-responsive nanocarrier for gemcitabine release on MCF–7 human breast cancer cells. Bioorg Chem 2022;118:105467.

[126] Chen X, Huang Y, Chen H, Chen Z, Chen J, Wang H, et al. Augmented EPR effect post IRFA to enhance the therapeutic efficacy of arsenic loaded ZIF-8 nanoparticles on residual HCC progression. J Nanobiotechnol 2022;20:1–18.

[127] Wang C, Zhao P, Yang G, Chen X, Jiang Y, Jiang X, et al. Reconstructing the intracellular pH microenvironment for enhancing photodynamic therapy. Mater Horiz 2020;7:1180–5.

[128] Guo H, Liu L, Hu Q, Dou H. Monodisperse ZIF-8@dextran nanoparticles co-loaded with hydrophilic and hydrophobic functional cargos for combined near-infrared fluorescence imaging and photothermal therapy. Acta Biomater 2022;137:290–304.

[129] Alsaiari SK, Qutub SS, Sun S, Baslyman W, Aldehaiman M, Alyami M, et al. Sustained and targeted delivery of checkpoint inhibitors by metal-organic frameworks for cancer immunotherapy. Sci Adv 2021;7:eabe7174.

[130] Jiang C, Zhang L, Xu X, Qi M, Zhang J, He S, et al. Engineering a smart agent for enhanced immunotherapy effect by simultaneously blocking PD-L1 and CTLA-4. Adv Sci 2021;8:2102500.

[131] Zhong X, Zhang Y, Tan L, Zheng T, Hou Y, Hong X, et al. An aluminum adjuvant-integrated nano-MOF as antigen delivery system to induce strong humoral and cellular immune responses. J Control Release 2019;300:81–92.

[132] Alyami MZ, Alsaiari SK, Li Y, Qutub SS, Aleisa FA, Sougrat R, et al. Cell-type-specific CRISPR/Cas9 delivery by biomimetic metal organic frameworks. J Am Chem Soc 2020;142:1715–20.

[133] Zhang M, Huang Y, Zou J, Yang Y, Yao Y, Cheng G, et al. Advanced oxidation nanoprocessing boosts immunogenicity of whole tumor cells. Advanced Science 2023;10:2302250.

[134] Pagani M, Bavbek S, Alvarez-Cuesta E, Berna Dursun A, Bonadonna P, Castells M, et al. Hypersensitivity reactions to chemotherapy: an EAACI Position Paper. Allergy 2022;77:388–403.

[135] Park SB, Goldstein D, Krishnan AV, Lin CS-Y, Friedlander ML, Cassidy J, et al. Chemotherapy-induced peripheral neurotoxicity: a critical analysis. CA Cancer J. Clin 2013;63:419–37.

[136] Lu H, Zhu S, Qian L, Xiang D, Zhang W, Nie A, et al. Activated expression of the chemokine Mig after chemotherapy contributes to chemotherapy-induced bone marrow suppression and lethal toxicity. Blood 2012;119:4868–77.

[137] Kamal NAMA, Abdulmalek E, Fakurazi S, Cordova KE, Rahman MBA. Surface peptide functionalization of zeolitic imidazolate framework-8 for autonomous homing and enhanced delivery of chemotherapeutic agent to lung tumor cells. Dalton Trans 2021;50:2375–86.

[138] Minotti G, Menna P, Salvatorelli E, Cairo G, Gianni L. Anthracyclines: molecular advances and pharmacologic developments in antitumor activity and cardiotoxicity. Pharmacol Rev 2004;56:185–229.

[139] Song Y, Han S, Liu S, Sun R, Zhao L, Yan C. Biodegradable imprinted polymer based on ZIF-8/DOX-HA for synergistically targeting prostate cancer cells and controlled drug release with multiple responses. ACS Appl Mater Interfaces 2023;15:25339–53.

[140] Longley DB, Harkin DP, Johnston PG. 5-Fluorouracil: mechanisms of action and clinical strategies. Nat Rev Cancer 2003;3:330–8.

[141] Kelland L. The resurgence of platinum-based cancer chemotherapy. Nat Rev Cancer 2007;7:573–84.

[142] Zheng Q, Liu X, Zheng Y, Yeung KWK, Cui Z, Liang Y, et al. The recent progress on metal-organic frameworks for phototherapy. Chem Soc Rev 2021;50:5086–125.

[143] Chen J, Ning C, Zhou Z, Yu P, Zhu Y, Tan G, et al. Nanomaterials as photothermal therapeutic agents. Prog Mater Sci 2019;99:1–26.

[144] Wang T, Li S, Zou Z, Hai L, Yang X, Jia X, et al. A zeolitic imidazolate framework-8-based indocyanine green theranostic agent for infrared fluorescence imaging and photothermal therapy. J Mater Chem B 2018;6:3914–21.

[145] Chen TT, Yi JT, Zhao YY, Chu X. Biomineralized metal-organic framework nanoparticles enable intracellular delivery and endo-lysosomal release of native active proteins. J Am Chem Soc 2018;140:9912–20.

[146] Meng X, Wang L, Zhao N, Zhao D, Shen Y, Yao Y, et al. Stimuli-responsive cancer nanomedicines inhibit glycolysis and impair redox homeostasis. Acta Biomater 2023;167:374–86.

[147] Wang HX, Li M, Lee CM, Chakraborty S, Kim HW, Bao G, et al. CRISPR/Cas9-based genome editing for disease modeling and therapy: challenges and opportunities for nonviral delivery. Chem Rev 2017;117:9874–906.

[148] Szebényi K, Füredi A, Bajtai E, Sama SN, Csiszar A, Gombos B, et al. Effective targeting of breast cancer by the inhibition of P-glycoprotein mediated removal of toxic lipid peroxidation byproducts from drug tolerant persister cells. Drug Resist Updat 2023;71:101007.

[149] Nasseri B, Alizadeh E, Bani F, Davaran S, Akbarzadeh A, Rabiee N, et al. Nanomaterials for photothermal and photodynamic cancer therapy. Appl Phys Rev 2022;9:011317.

[150] Lu S, Tian H, Li L, Li B, Yang M, Zhou L, et al. Nanoengineering a zeolitic imidazolate framework-8 capable of manipulating energy metabolism against cancer chemo-phototherapy resistance. Small 2022;18:2204926.

[151] Chen MM, Hao HL, Zhao W, Zhao X, Chen HY, Xu JJ. A plasmon-enhanced theranostic nanoplatform for synergistic chemo-phototherapy of hypoxic tumors in the NIR-II window. Chem Sci 2021;12:10848–54.

[152] Zhang W, Chen L, Zhang X, Gong P, Wang X, Xu Z, et al. Functionalized nanohybrids with rod shape for improved chemo-phototherapeutic effect against cancer by sequentially generating singlet oxygen and carbon dioxide bubbles. Biomater Sci 2023;11:6894–905.

[153] Xu M, Hu Y, Ding W, Li F, Lin J, Wu M, et al. Rationally designed rapamycin-encapsulated ZIF-8 nanosystem for overcoming chemotherapy resistance. Biomaterials 2020;258:120308.

[154] Zhou S, Shang Q, Ji J, Luan Y. A nanoplatform to amplify apoptosis-to-pyroptosis immunotherapy via immunomodulation of myeloid-derived suppressor cells. ACS Appl Mater Interfaces 2021;13:47407–17.

[155] Feng J, Yu W, Xu Z, Wang F. An intelligent ZIF-8-gated polydopamine nanoplatform for in vivo cooperatively enhanced combination phototherapy. Chem Sci 2020;11:1649–56.

[156] Wei X, Huang H, Guo J, Li N, Li Q, Zhao T, et al. Biomimetic nano-immunoactivator via ionic metabolic modulation for strengthened NIR-II photothermal immunotherapy. Small 2023;19:2304370.

[157] Chen D, Suo M, Guo J, Tang W, Jiang W, Liu Y, et al. Development of MOF "armor-plated" phycocyanin and synergistic inhibition of cellular respiration for hypoxic photodynamic therapy in patient-derived xenograft models. Adv Healthc Mater 2021;10:e2001577.

[158] Wang Y, Wang H, Song Y, Lv M, Mao Y, Song H, et al. IR792-MCN@ZIF-8-PD-L1 siRNA drug delivery system enhances photothermal immunotherapy for triple-negative breast cancer under near-infrared laser irradiation. J Nanobiotechnology 2022;20:96.

[159] Geng L, Lu T, Jing H, Zhou Y, Liang X, Li J, et al. Iron-based and BRD4-downregulated strategy for amplified ferroptosis based on pH-sensitive/NIR-II-boosted nano-matchbox. Acta Pharm. Sin. B 2023;13:863–78.

[160] Wang H, Chen Y, Wang H, Liu X, Zhou X, Wang F. DNAzyme-loaded metal-organic frameworks (MOFs) for self-sufficient gene therapy. Angew Chem Int Ed 2019;58:7380–4.

[161] Zhao X, Cheng H, Wang Q, Nie W, Yang Y, Yang X, et al. Regulating photosensitizer metabolism with DNAzyme-loaded nanoparticles for amplified mitochondria-targeting photodynamic immunotherapy. ACS Nano 2023;17:13746–59.

[162] Zhang C, Zhang L, Wu W, Gao F, Li RQ, Song W, et al. Artificial super neutrophils for inflammation targeting and HClO generation against tumors and infections. Adv Mater 2019;31:e1901179.

[163] Xiao X, Liang S, Zhao Y, Pang M, Ma P, Cheng Z, et al. Multifunctional carbon monoxide nanogenerator as immunogenic cell death drugs with enhanced antitumor immunity and antimetastatic effect. Biomaterials 2021;277:121120.

[164] Liang Y, Li M, Huang Y, Guo B. An integrated strategy for rapid hemostasis during tumor resection and prevention of postoperative tumor recurrence of hepatocellular carcinoma by antibacterial shape memory cryogel. Small 2021;17:e2101356.

[165] An J, Hu YG, Li C, Hou XL, Cheng K, Zhang B, et al. A pH/ultrasound dual-response biomimetic nanoplatform for nitric oxide gas-sonodynamic combined therapy and repeated ultrasound for relieving hypoxia. Biomaterials 2020;230:119636.

[166] Zeng X, Chen B, Song Y, Lin X, Zhou SF, Zhan G. Fabrication of versatile hollow metal-organic framework nanoplatforms for folate-targeted and combined cancer imaging and therapy. ACS Appl Bio Mater 2021;4:6417–29.

[167] Wang Q, Niu D, Shi J, Wang L. A three-in-one ZIFs-derived CuCo(O)/GOx@PCNs hybrid cascade nanozyme for immunotherapy/enhanced starvation/photothermal therapy. ACS Appl Mater Interfaces 2021;13:11683–95.

[168] Chen Q, Deng B, Luo Q, Song G. Deep tumor-penetrated nanosystem eliminates cancer stem cell for highly efficient liver cancer therapy. Chem Eng J 2021;421:127874.

[169] Chen J, Bao Y, Song Y, Zhang C, Qiu F, Sun Y, et al. Hypoxia-alleviated nanoplatform to enhance chemosensitivity and sonodynamic effect in pancreatic cancer. Cancer Lett 2021;520:100–8.

[170] Chen QW, Liu XH, Fan JX, Peng SY, Wang JW, Wang XN, et al. Self-mineralized photothermal bacteria hybridizing with mitochondria-targeted metal-organic frameworks for augmenting photothermal tumor therapy. Adv Funct Mater 2020;30:1909806.

[171] Shen J, Yu H, Shu Y, Ma M, Chen H. A robust ROS generation strategy for enhanced chemodynamic/photodynamic therapy via H_2O_2/O_2 self-supply and Ca^{2+} overloading. Adv Funct Mater 2021;31:2106106.

[172] Yang X, Tang Q, Jiang Y, Zhang M, Wang M, Mao L. Nanoscale ATP-responsive zeolitic imidazole framework-90 as a general platform for cytosolic protein delivery and genome editing. J Am Chem Soc 2019;141:3782–6.

[173] Fu J, Zhu X, Zhao J, Cai J, Yang X, Zhang Y, et al. A NIR-laser smart stimulus self-assembly nanosystem with acid-activatable for enhanced photothermal and chemotherapy against tumors. Mater. Today Chem. 2023;34:101776.

[174] Wang Q, Yu Y, Chang Y, Xu X, Wu M, Ediriweera GR, et al. Fluoropolymer-MOF hybrids with switchable hydrophilicity for ^{19}F MRI-monitored cancer therapy. ACS Nano 2023;17:8483–98.

[175] Wang L, Xu Y, Liu C, Si W, Wang W, Zhang Y, et al. Copper-doped MOF-based nanocomposite for GSH depleted chemo/photothermal/chemodynamic combination therapy. Chem Eng J 2022;438:135567.

[176] Jing X, Yang F, Shao C, Wei K, Xie M, Shen H, et al. Role of hypoxia in cancer therapy by regulating the tumor microenvironment. Mol Cancer 2019;18:157.

[177] Fang C, Cen D, Wang Y, Wu Y, Cai X, Li X, et al. ZnS@ZIF-8 core-shell nanoparticles incorporated with ICG and TPZ to enable H$_2$S-amplified synergistic therapy. Theranostics 2020;10:7671–82.

[178] Tan G, Zhong Y, Yang L, Jiang Y, Liu J, Ren F. A multifunctional MOF-based nanohybrid as injectable implant platform for drug synergistic oral cancer therapy. Chem Eng J 2020;390:124446.

[179] Holohan C, Van Schaeybroeck S, Longley DB, Johnston PG. Cancer drug resistance: an evolving paradigm. Nat Rev Cancer 2013;13:714–26.

[180] Robey RW, Pluchino KM, Hall MD, Fojo AT, Bates SE, Gottesman MM. Revisiting the role of ABC transporters in multidrug-resistant cancer. Nat Rev Cancer 2018;18:452–464.

[181] Liu G, Wang L, Liu J, Lu L, Mo D, Li K, et al. Engineering of a core-shell nanoplatform to overcome multidrug resistance via ATP deprivation. Adv Healthc Mater 2020;9:2000432.

[182] Ma L, Zhou J, Wu Q, Luo G, Zhao M, Zhong G, et al. Multifunctional 3D-printed scaffolds eradiate orthotopic osteosarcoma and promote osteogenesis via microwave thermo-chemotherapy combined with immunotherapy. Biomaterials 2023;301:122236.

[183] Zhang Y, Yang Y, Shi J, Wang L. A multimodal strategy of Fe$_3$O$_4$@ZIF-8/GOx@MnO$_2$ hybrid nanozyme via TME modulation for tumor therapy. Nanoscale 2021;13:16571–88.

[184] Cheng Q, Gao F, Yu WY, Zou MZ, Ding XL, Li MJ, et al. Near-infrared triggered cascade of antitumor immune responses based on the integrated core-shell nanoparticle. Adv Funct 2020;30:2000335.

[185] Liu Y, Wu H, Wang S, Zhang X, Gong L, Xiao C, et al. Biomimetic multifunctional nanodrugs enable regulating abnormal tumor metabolism and amplifying PDT-induced immunotherapy for synergistically enhanced tumor ablation. Mater Today 2023;68:125–47.

[186] Yu F, Wang T, Wang Y, Liu T, Xiong H, Liu L, et al. Nanozyme-nanoclusters in metal-organic framework: GSH triggered Fenton reaction for imaging guided synergistic chemodynamic-photothermal therapy. Chem. Eng. J. 2023;472:144910.

[187] Irvine DJ, Dane EL. Enhancing cancer immunotherapy with nanomedicine. Nat Rev Immunol 2020;20:321–34.

[188] Li K, Xu K, He Y, Yang Y, Tan M, Mao Y, et al. Oxygen self-generating nanoreactor mediated ferroptosis activation and immunotherapy in triple-negative breast cancer. ACS Nano 2023;17:4667–87.

[189] Ge YX, Zhang TW, Zhou L, Ding W, Liang HF, Hu ZC, et al. Enhancement of anti-PD-1/PD-L1 immunotherapy for osteosarcoma using an intelligent autophagy-controlling metal organic framework. Biomaterials 2022;282:121407.

[190] Sun L, Gao H, Wang H, Zhou J, Ji X, Jiao Y, et al. Nanoscale metal-organic frameworks-mediated degradation of mutant p53 proteins and activation of cGAS-STING pathway for enhanced cancer immunotherapy. Advanced Science 2024:2307278.

[191] Fang X, Chen Z, Zhou W, Li T, Wang M, Gao Y, et al. Boosting glioblastoma therapy with targeted pyroptosis induction. Small 2023;19:2207604.

[192] Ding B, Chen H, Tan J, Meng Q, Zheng P, Ma P, et al. ZIF-8 nanoparticles evoke pyroptosis for high-efficiency cancer immunotherapy. Angew Chem Int Ed 2023;62:e202215307.

[193] Wang M, Wang D, Chen Q, Li C, Li Z, Lin J. Recent advances in glucose-oxidase-based nanocomposites for tumor therapy. Small 2019;15:1903895.

[194] Yu J, Wei Z, Li Q, Wan F, Chao Z, Zhang X, et al. Advanced cancer starvation therapy by simultaneous deprivation of lactate and glucose using a MOF nanoplatform. Adv Sci 2021;8:2101467.

[195] Son S, Kim JH, Wang X, Zhang C, Yoon SA, Shin J, et al. Multifunctional sonosensitizers in sonodynamic cancer therapy. Chem Soc Rev 2020:49.

[196] Zhou Y, Hu K, Zhang FQ. Adjuvant concurrent chemoradiotherapy *vs.* radiotherapy alone in cervical cancer patients with intermediate-risk factors after radical surgery. Int. J. Radiat. Oncol. Biol. Phys. 2023;117:e560.

[197] Wang Y, Zhang H, Liu Y, Younis MH, Cai W, Bu W. Catalytic radiosensitization: insights from materials physicochemistry. Materials Today 2022;57:262–78.

[198] Pan S, Huang G, Sun Z, Chen X, Xiang X, Jiang W, et al. X-Ray-eesponsive zeolitic imidazolate framework-capped nanotherapeutics for cervical cancer-targeting radiosensitization. Adv. Funct. Mater. 2023;33:2213364.

[199] Wu Q, Li M, Tan L, Yu J, Chen Z, Su L, et al. A tumor treatment strategy based on biodegradable BSA@ZIF-8 for simultaneously ablating tumors and inhibiting infection. Nanoscale Horiz 2018;3:606–15.

[200] Luo D, Wang X, Luo X, Wu S. Low-dose of zeolitic imidazolate framework-8 nanoparticle cause energy metabolism disorder through lysosome-mitochondria dysfunction. Toxicology 2023;489:153473.

[201] Hoop M, Walde CF, Riccò R, Mushtaq F, Terzopoulou A, Chen X-Z, et al. Biocompatibility characteristics of the metal organic framework ZIF-8 for therapeutical applications. Appl Mater Today 2018;11:13–21.

[202] Zhao H, Li T, Yao C, Gu Z, Liu C, Li J, et al. Dual roles of metal-organic frameworks as nanocarriers for miRNA delivery and adjuvants for chemodynamic therapy. ACS Appl Mater Interfaces 2021;13:6034–42.

[203] Chen P, He M, Chen B, Hu B. Size- and dose-dependent cytotoxicity of ZIF-8 based on single cell analysis. Ecotoxicol Environ Saf 2020;205:111110.

[204] Kota D, Kang L, Rickel A, Liu J, Smith S, Hong Z, et al. Low doses of zeolitic imidazolate framework-8 nanoparticles alter the actin organization and contractility of vascular smooth muscle cells. J Hazard Mater 2021;414:125514.

[205] Hao F, Yan X-P. Nano-sized zeolite-like metal-organic frameworks induced hematological effects on red blood cell. J Hazard Mater 2022;424:127353.

[206] Ettlinger R, Lächelt U, Gref R, Horcajada P, Lammers T, Serre C, et al. Toxicity of metal–organic framework nanoparticles: from essential analyses to potential applications. Chem Soc Rev 2022;51:464–84.

[207] Prabhu R, Mohamed Asik R, Anjali R, Archunan G, Prabhu NM, Pugazhendhi A, et al. Ecofriendly one pot fabrication of methyl gallate@ZIF-L nanoscale hybrid as pH responsive drug delivery system for lung cancer therapy. Process Biochem 2019;84:39–52.

[208] Li C, Ye J, Yang X, Liu S, Zhang Z, Wang J, et al. Fe/Mn bimetal-doped ZIF-8-coated luminescent nanoparticles

with up/downconversion dual-mode emission for tumor self-Enhanced NIR-II imaging and catalytic therapy. ACS Nano 2022;16:18143–56.

[209] Deng S, Yan X, Xiong P, Li G, Ku T, Liu N, et al. Nanoscale cobalt-based metal-organic framework impairs learning and memory ability without noticeable general toxicity: first *in vivo* evidence. Sci Total Environ 2021;771: 145063.

[210] Foglietta F, Serpe L, Canaparo R. The effective combination between 3D cancer models and stimuli-responsive nanoscale drug delivery systems. Cells 2021;10:3295.

[211] Wei K, He M, Zhang J, Zhao C, Nie C, Zhang T, et al. A DNA logic circuit equipped with a biological amplifier loaded into biomimetic ZIF-8 nanoparticles enables accurate identification of specific cancers *in vivo*. Angew Chem Int Ed 2023;62:e202307025.